



UvA-DARE (Digital Academic Repository)

The discovery of GluA3-dependent synaptic plasticity

Renner, M.C.

Publication date

2016

Document Version

Final published version

[Link to publication](#)

Citation for published version (APA):

Renner, M. C. (2016). *The discovery of GluA3-dependent synaptic plasticity*. [Thesis, fully internal, Universiteit van Amsterdam]. Uitgeverij BOXPress.

General rights

It is not permitted to download or to forward/distribute the text or part of it without the consent of the author(s) and/or copyright holder(s), other than for strictly personal, individual use, unless the work is under an open content license (like Creative Commons).

Disclaimer/Complaints regulations

If you believe that digital publication of certain material infringes any of your rights or (privacy) interests, please let the Library know, stating your reasons. In case of a legitimate complaint, the Library will make the material inaccessible and/or remove it from the website. Please Ask the Library: <https://uba.uva.nl/en/contact>, or a letter to: Library of the University of Amsterdam, Secretariat, P.O. Box 19185, 1000 GD Amsterdam, The Netherlands. You will be contacted as soon as possible.

Chapter 2

Synaptic plasticity through activation of AMPA-receptor subunit GluA3

Maria C. Renner, Eva H.H. Albers, Nicolas Gutierrez-Castellanos, Tessa R. Lodder,
Niels R. Reinders, Chris I. De Zeeuw and Helmut W. Kessels.

Submitted.

ABSTRACT

AMPA receptors are responsible for fast excitatory synaptic transmission in the brain. In CA1 pyramidal neurons of the hippocampus two types of AMPA receptors predominate: those that contain subunits GluA1 and GluA2, and those that contain GluA3 and GluA2. GluA1-containing AMPA receptors have been extensively studied and are known to play a key role in several forms of synaptic plasticity and memory formation. In contrast, the contribution of GluA3 to synapse physiology has remained elusive. Here we show that under basal conditions GluA3-containing AMPA receptors are inactive and contribute little to synaptic currents. During fear, a rise in intracellular cyclic AMP levels driven by norepinephrine release restores GluA3 channel function, leading to a massive and transient synaptic potentiation. Our results indicate that GluA3- and GluA1-containing AMPA receptors contribute differently to synaptic plasticity and memory formation.

INTRODUCTION

Memory formation involves the selective strengthening of groups of synapses within neuronal circuits that are activated during an experience. The encoding of memories is thought to depend on the long-term potentiation (LTP) and long-term depression (LTD) of synaptic strength (Whitlock et al., 2006; Nabavi et al., 2014). LTP and LTD can be expressed by a change in the number of postsynaptic AMPA-type glutamate receptors (AMPA receptors) (Huganir and Nicoll 2013; Malinow and Malenka 2002). AMPAR channels are formed through the assembly of four AMPAR subunits. In excitatory neurons of the mature hippocampus, the majority of AMPARs consist of subunits GluA1 and GluA2 (GluA1/2 heteromers) or GluA2 and GluA3 (GluA2/3 heteromers) (Wenthold et al., 1996).

GluA1-containing AMPARs play an essential role in several forms of experience-dependent plasticity (Kessels and Malinow 2009). GluA1 is inserted into synapses upon the induction of LTP or the formation of fear memories, whereas a selective blockade of GluA1 trafficking impairs LTP and memory formation (Mitsushima et al., 2011; Rumpel et al., 2005). In line with this, LTP and the formation of fear memories are severely impaired in GluA1-deficient mice (Humeau et al., 2007). In contrast to the short cytoplasmic tails (C-tails) of GluA2 or GluA3, the GluA1 subunit has a long C-tail that contains several unique phosphorylation sites by which the trafficking of

GluA1 to synapses can be regulated. For instance, the C-tail of GluA1 can be phosphorylated by protein kinase A (PKA), which in turn promotes the surface expression of GluA1-containing AMPARs (Joiner et al., 2010; Man et al., 2007), thereby lowering the threshold for LTP and facilitating the formation of memories (Crombag et al., 2008; Hu et al., 2007; Qian et al., 2012). Such activation by PKA can occur following activation of beta-adrenergic receptors (β -ARs) by norepinephrine (NE), which leads to activation of adenylyl cyclases, producing a rise in intracellular cyclic AMP (cAMP) (Hall 2004; Vanhoose and Winder 2003). Whereas the role of GluA1 in synaptic plasticity and learning is well established, the role of GluA3-containing AMPARs has remained unclear. In hippocampal neurons that lack GluA3 LTP and LTD are intact (Meng et al., 2003) and the capacity of GluA3-deficient mice to acquire fear memories is comparable to wild-type congenics (Adamczyk et al., 2012; Humeau et al., 2007).

There are currently two theories on the relevance of having two different types of AMPARs in excitatory neurons. One model dictates that LTP and learning involve synaptic trafficking of GluA1-containing AMPARs, whereas GluA3-containing AMPARs are constitutively replacing AMPARs at synapses independently of neuronal activity (Kessels and Malinow, 2009; Shi et al., 2001). In this model GluA3-containing AMPARs are hypothesized to play a homeostatic role in keeping synapse strength stable in the face of protein turnover (McCormack et al., 2006). The second model states that in essence any type of AMPAR can be inserted into synapses upon LTP induction (Granger et al., 2013) and therefore AMPARs can contribute to learning in a manner independent of subunit composition. In this model the observation that GluA1-containing AMPARs dominate in mediating synaptic strengthening is explained by the notion that GluA3-containing AMPARs contribute little to synaptic and extrasynaptic AMPAR currents in hippocampal pyramidal cells (Lu et al., 2009).

In the present study we combine these two models by showing that although GluA3-containing AMPARs are present at hippocampal synapses in substantial numbers, they transmit no or little currents upon glutamate binding under basal conditions. However, when activation of β -ARs following fear results in an increase in intracellular cAMP, GluA3-containing AMPARs become functional, leading to synaptic potentiation in a novel format. Yet interestingly, when GluA3-containing AMPARs are contributing substantially to synaptic currents, they play no part in hippocampus-dependent memory formation.

RESULTS

A rise in cAMP increases the open-channel probability of GluA3-containing AMPARs

To examine the contribution of GluA3 to the pool of extrasynaptic AMPARs, we recorded currents evoked by puffing AMPA onto outside-out membrane patches excised from cell bodies of CA1 pyramidal neurons in organotypic hippocampal slices prepared from wild-type, GluA3-deficient or GluA1-deficient mice. The absence of GluA3 had no effect on extrasynaptic AMPAR currents ($p > 0.9$, Figure 1A). A non-stationary noise analysis on these outside-out AMPAR currents showed that the absence of GluA3-containing AMPAR currents did not result in differences in the average number of functional AMPARs per patch, single channel conductance or open-channel probability (Figure C,D). Consistent with previous results (Andrásfalvy et al., 2003), GluA1-deficient outside-out patches contained relatively few functional AMPAR channels, and those that were present had a low single-channel conductance and open channel probability (Figure C,D). As a result, currents were 83% smaller in GluA1-deficient outside-out patches compared with those that contained GluA1 ($p < 0.0001$, Figure 1A). These data indicate that under basal conditions the majority of extrasynaptic AMPAR currents are derived from GluA1-containing AMPARs.

A rise in intracellular cAMP results in a long-lasting potentiation of AMPAR currents (Carroll et al., 1998; Chavez-Noriega and Stevens, 1992; Sokolova et al., 2006). To study how cAMP modifies AMPARs, we recorded AMPA-evoked currents from outside-out patches with or without cAMP in the solution of the recording pipette, while blocking cAMP degradation by phosphodiesterases (PDEs) with IBMX (Figure 1A). We note that IBMX by itself did not change the amplitude of the response to AMPA puffs (Figure S1A). In somatic membrane patches from wild-type neurons the amplitudes of the responses to AMPA puffs were 2-fold higher in the presence of cAMP ($p = 0.0009$; Figure 1A). In patches from GluA3-deficient somatic patches cAMP did not change AMPAR currents ($p = 0.9$; Figure 1A). However, in GluA1-deficient CA1 patches AMPAR currents increased 4.5-fold in the presence of cAMP ($p < 0.0001$; Figure 1A). This occurred as a function of an increase in the estimated number of functional channels ($p = 0.0009$), channel conductance ($p = 0.04$) and open-channel probability ($p = 0.002$; Figure 1C,D). As a result, GluA3-containing AMPARs activated by cAMP reached conductance levels comparable to those of GluA1-containing AMPARs in GluA3-deficient patches ($p = 0.9$), the channel properties of

which were not modified by cAMP (Figure 1C,D). These experiments suggest that cAMP selectively potentiated currents through GluA3-containing AMPARs, revealing a novel type of AMPAR plasticity.

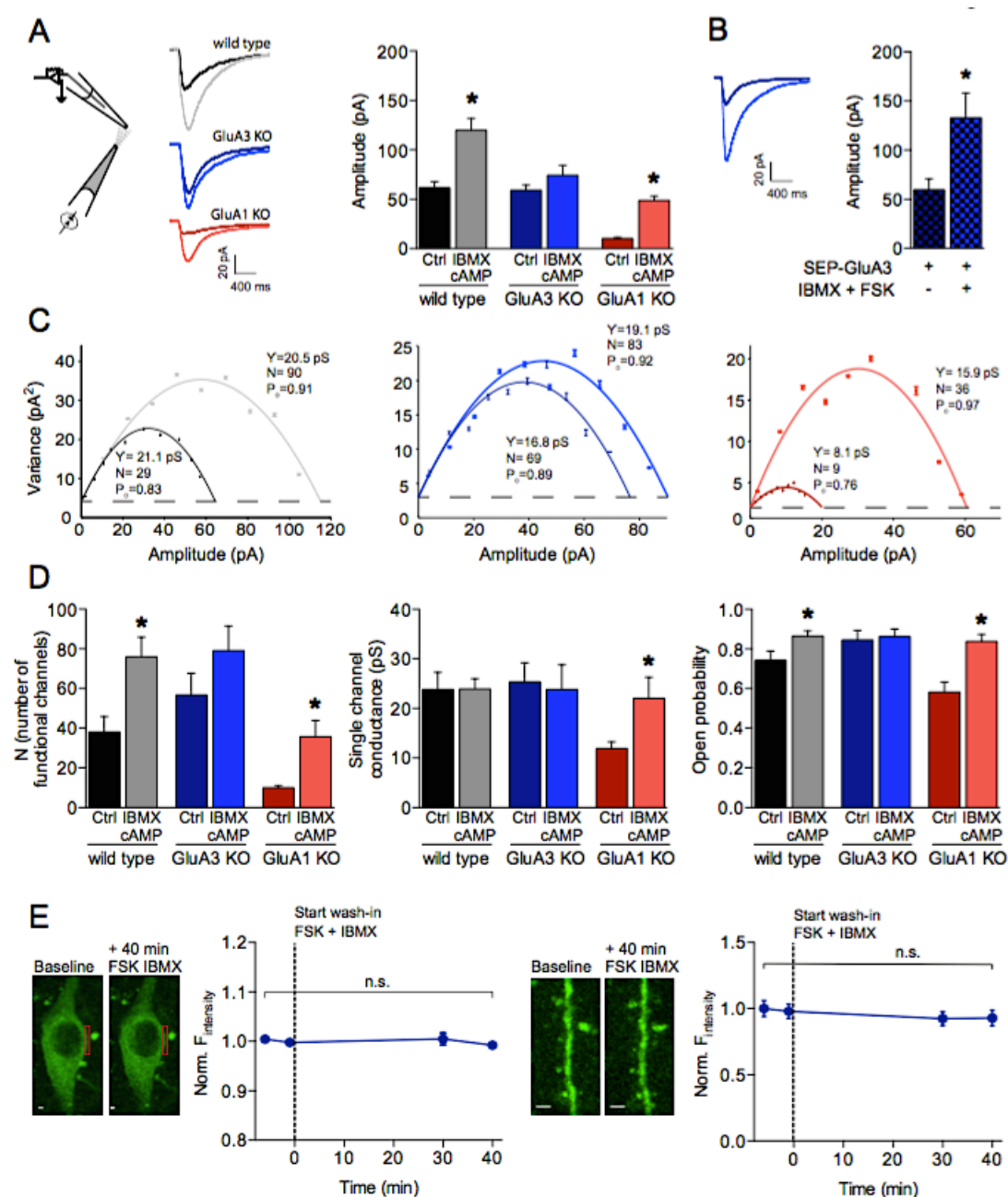


Figure 1. cAMP increases currents but not the number of GluA3-containing AMPARs at the cell surface

(A) Experimental setup, example traces and averages of AMPAR amplitudes in response to AMPA puffs onto outside-out patches from WT (CA1 cell bodies without (black; n=15) or with (gray; n=24) cAMP in pipette, GluA3-KO without (dark blue; n=20) or with (light blue; n=20) cAMP, and GluA1-KO without (dark red; n=18) or with (light red; n=10) cAMP. All recordings in the presence of desensitization blockers cyclothiazide and PEPA and cAMP condition in the presence of PDE inhibitor IBMX. (B) Sindbis expression of SEP-GluA3 rescues the

cAMP-driven GluA3-plasticity. Outside-out patches from SEP-GluA3 infected GluA3-KO cell bodies, before (n=7) and after (n=8) wash-in of forskolin plus IBMX. (C) Example graphs of non-stationary noise analysis for WT, GluA3-KO and GluA1-KO outside-out recordings. (D) Average number of functional channels, single channel conductance and open probability extracted from non-stationary noise analysis of the outside-out recordings (see methods). (E) Example images and average fluorescence intensity of GluA3-KO cell bodies (left; n=6) and dendrites (right; n=8) infected with SEP-GluA3 visualized with 2-photon laser scanning microscopy before and after wash-in of forskolin plus IBMX (n=8). Scale bars indicate 5 μm . Error bars indicate SEM, * indicates $p < 0.05$.

To examine whether GluA3-plasticity involves trafficking of GluA3 to the cell surface, we introduced fluorescently labeled GluA3 into GluA3-deficient CA1 neurons. Whereas recombinant GluA3 expression did not alter outside-out AMPAR currents, washing-in both the adenylyl cyclase activator forskolin and PDE inhibitor IBMX rescued the cAMP-driven potentiation of AMPAR currents ($p=0.03$; Figure 1B), indicating that recombinant GluA3 responds similarly to a rise in cAMP as endogenous GluA3. As a means to quantify the surface levels of recombinant GluA3, the subunit was tagged with super ecliptic phluorin (SEP), which is only fluorescent at neutral pH, i.e. when present in the ER, cis-Golgi or at the cell surface, but not at acidic pH in late endosomes or lysosomes. We visualized the pH-sensitivity of SEP-GluA3 by acutely washing in ACSF buffered at pH 5 (Figure S1B). Upon the wash-in of forskolin and IBMX, the SEP fluorescence levels remained unchanged at the surface area of both dendrites ($p=0.4$) and cell bodies ($p=0.2$; Figure 1E), suggesting that cAMP-driven GluA3-plasticity does not result from trafficking of GluA3-containing AMPARs from endocytic compartments to the cell surface.

We next examined the cAMP-driven activation of GluA3 channel function by performing single-channel recordings under cell-attached configuration from soma of CA1 pyramidal GluA1- or GluA3-deficient neurons from organotypic hippocampal slices, while adding AMPA to the recording pipette. Single-channel AMPAR currents from GluA3-deficient neurons did not change in the presence of forskolin (Figure 2A-E), indicating that the channel properties of GluA1-containing AMPARs remained unchanged upon a rise in cAMP. In GluA1-deficient neurons the basal open probability of AMPARs was low and events were almost exclusively in open state 1, which occurs when only two out of four subunits change conformation upon glutamate binding. In the presence of forskolin the open probability increased substantially ($p=0.0001$; Figure 2F,G) and GluA3-containing AMPARs more often reached open states 2 and 3 (open state 1: $p < 0.0001$, 2: $p=0.0002$, 3: $p < 0.0001$; Figure 2H), leading to enhanced average conductance ($p < 0.0001$; Figure 2I) without

modifying the conductance level of each open state (open state 1: $p=0.2$, 2: $p=0.06$, 3: $p=0.8$; Figure 2J). These experiments indicate that GluA3-containing AMPARs are largely electrically quiet under basal conditions, but become functional upon a rise in cAMP by increasing their capacity for glutamate-gated channel opening.

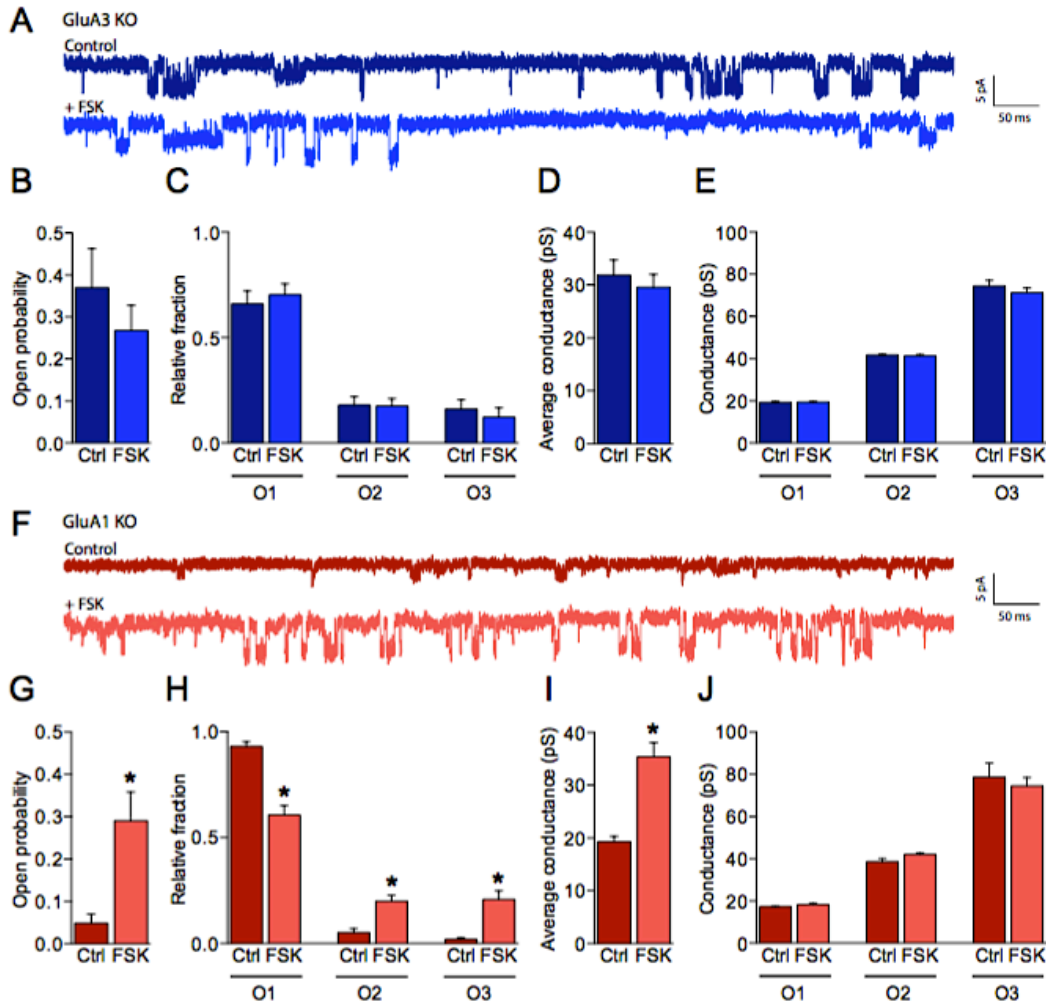


Figure 2. cAMP increases the open-channel probability of GluA3-containing AMPARs

(A-E) Single channel recordings under cell-attached configuration of GluA3-KO (blue) and (F-J) GluA1-KO (red) neurons in control conditions and incubated with forskolin (GluA3-KO ctrl: $n=15$, FSK: $n=14$; GluA1-KO ctrl: $n=15$, FSK $n=14$). Example traces (A,F), open probability (B,G), fraction of time spent in each open state (C,H), average conductance (D,I) and conductances of each open state (E,J). Error bars indicate SEM, * indicates $p<0.05$.

A rise in cAMP activates GluA2/3s at synapses

To investigate whether the cAMP-driven activation of GluA3-plasticity occurs at synapses, we performed whole-cell patch clamp recordings on CA1 neurons from organotypic hippocampal slices in the presence or absence of forskolin. Forskolin incubation significantly increased AMPAR/NMDAR ratios evoked by stimulating

Schaffer collateral inputs onto synapses of wild-type CA1 neurons ($p=0.01$; Figure 3A). In GluA3-deficient neurons forskolin failed to trigger a change in the AMPAR/NMDAR ratio ($p=0.6$; Figure 3A), indicating that forskolin activated GluA3-containing AMPARs at the postsynaptic membrane. Consistent with the notion that the potentiation effect of forskolin is expressed postsynaptically (Sokolova et al., 2006), forskolin did not affect presynaptic glutamate release, since paired pulse ratios (WT: $p=0.3$, KO: $p=0.7$; Figure 3B) and the quantal content of evoked glutamate release ($p=0.7$, Figure S2A) remained unchanged.

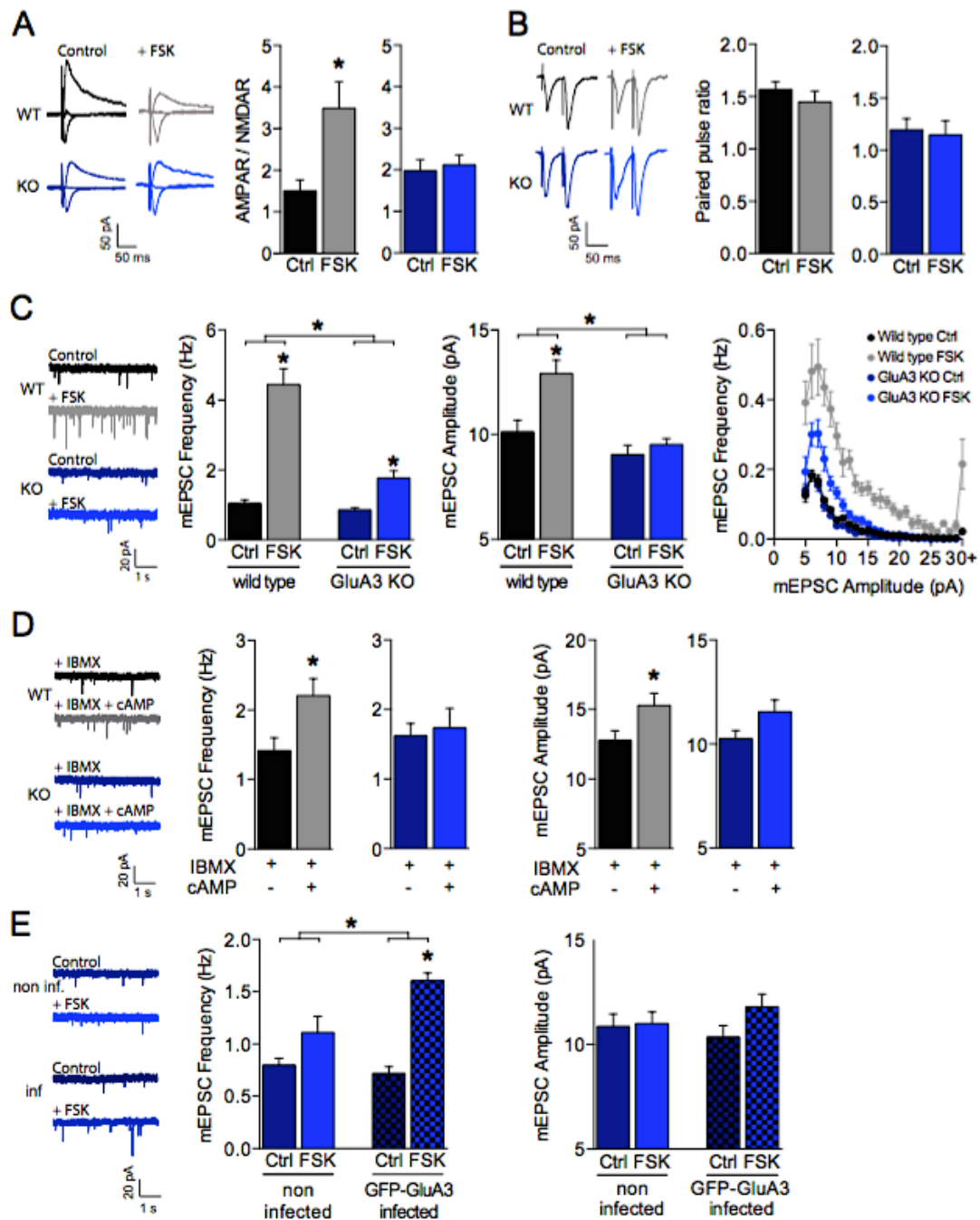


Figure 3. The cAMP-driven postsynaptic potentiation is dependent on GluA3

(A) Example traces and average AMPAR/NMDAR EPSC ratios of WT neurons with (n=13) or without (n=9) forskolin, and GluA3-KO neurons with (n=8) or without (n=8) forskolin. (B) Example traces and average paired pulsed ratio of WT CA1 neurons with (n=8) or without (n=8) forskolin, and of GluA3-KO neurons with (n=8) or without (n=8) forskolin. (C) Example traces, mEPSC frequencies, mEPSC amplitudes and mEPSC distribution per 1 pA binned amplitude of WT neurons with (n=10) or without (n=10) forskolin and GluA3-KO neurons with (n=10) or without (n=8) forskolin. (D) Example traces, mEPSC frequencies and mEPSC amplitudes in the presence of IBMX of WT neurons with (n=10) or without (n=11) cAMP and of GluA3-KO neurons with (n=8) or without (n=8) cAMP in recording pipette. (E) Example traces, mEPSC frequencies and mEPSC amplitudes in GluA3-KO slices of uninfected CA1 neurons with (n=9) or without (n=8) forskolin, and GFP-GluA3 infected neurons with (n=11) or without (n=8) forskolin. Error bars indicate SEM, * indicates $p < 0.05$.

In miniature EPSC (mEPSC) recordings, forskolin induced a modest increase in the average amplitude ($p=0.002$) and a large increase in the frequency ($p < 0.0001$) of mEPSC events (Figure 3C). A postsynaptic change in AMPAR currents reflected by a change in mEPSC frequency rather than mEPSC amplitude is not uncommon and has been observed previously (Lee et al., 2014; Lu et al., 2009; Rumbaugh et al., 2006). In GluA3-deficient neurons, forskolin did not change the average mEPSC amplitude and triggered a mEPSC frequency increase ($p=0.001$) that was significantly smaller in magnitude compared to that in wild-type CA1 neurons ($p=0.0005$; Figure 3C). GluA3-dependent synaptic potentiation was also induced by directly infusing cAMP into CA1 neurons with PDEs blocked by IBMX (WT: $p=0.01$, GluA3-KO: $p=0.8$; Figure 3D). Re-introducing GluA3 by acute viral expression of GFP-GluA3 in GluA3-deficient CA1 neurons rescued the forskolin-driven increase in mEPSC frequency ($p=0.001$; Figure 3E). These experiments indicate that the cAMP-mediated increase in postsynaptic AMPAR currents requires GluA3.

Neurons that are deficient in both GluA1 and GluA3 virtually lacked mEPSC events (Figure 4A), indicating that synaptic AMPAR currents recorded from GluA1-deficient CA1 neurons predominantly stem from GluA3-containing AMPARs. Whereas these GluA1/GluA3 double deficient neurons were insensitive to forskolin ($p > 0.9$), forskolin did elevate the mEPSC frequency in GluA1-deficient neurons ($p=0.0009$; Figure 4A). GluA3-containing AMPARs are thought to predominantly exist as GluA2/3 heteromers, because structural constraints at their N-terminal domain prevent GluA3s from efficiently forming homomers (Sukumaran et al., 2011). To test whether the forskolin-driven GluA3-plasticity was mediated by GluA2/3 heteromers, we measured the AMPAR rectification indices in GluA1-deficient neurons. Unlike GluA2-containing AMPARs, GluA2-lacking AMPARs are rectifying: they conduct only at negative potentials. GluA1-deficient neurons displayed no rectifying currents either

before or after forskolin treatment ($p=0.6$, Figure 4B), indicating that the cAMP-mediated increase in synaptic efficacy is produced by GluA2/3 heteromers.

A rise in cAMP can cause postsynaptic potentiation by triggering GluA1 phosphorylation via PKA activation (Joiner et al., 2010; Man et al., 2007). Indeed, adding the specific PKA activator N002 to the recording pipette increased mEPSC

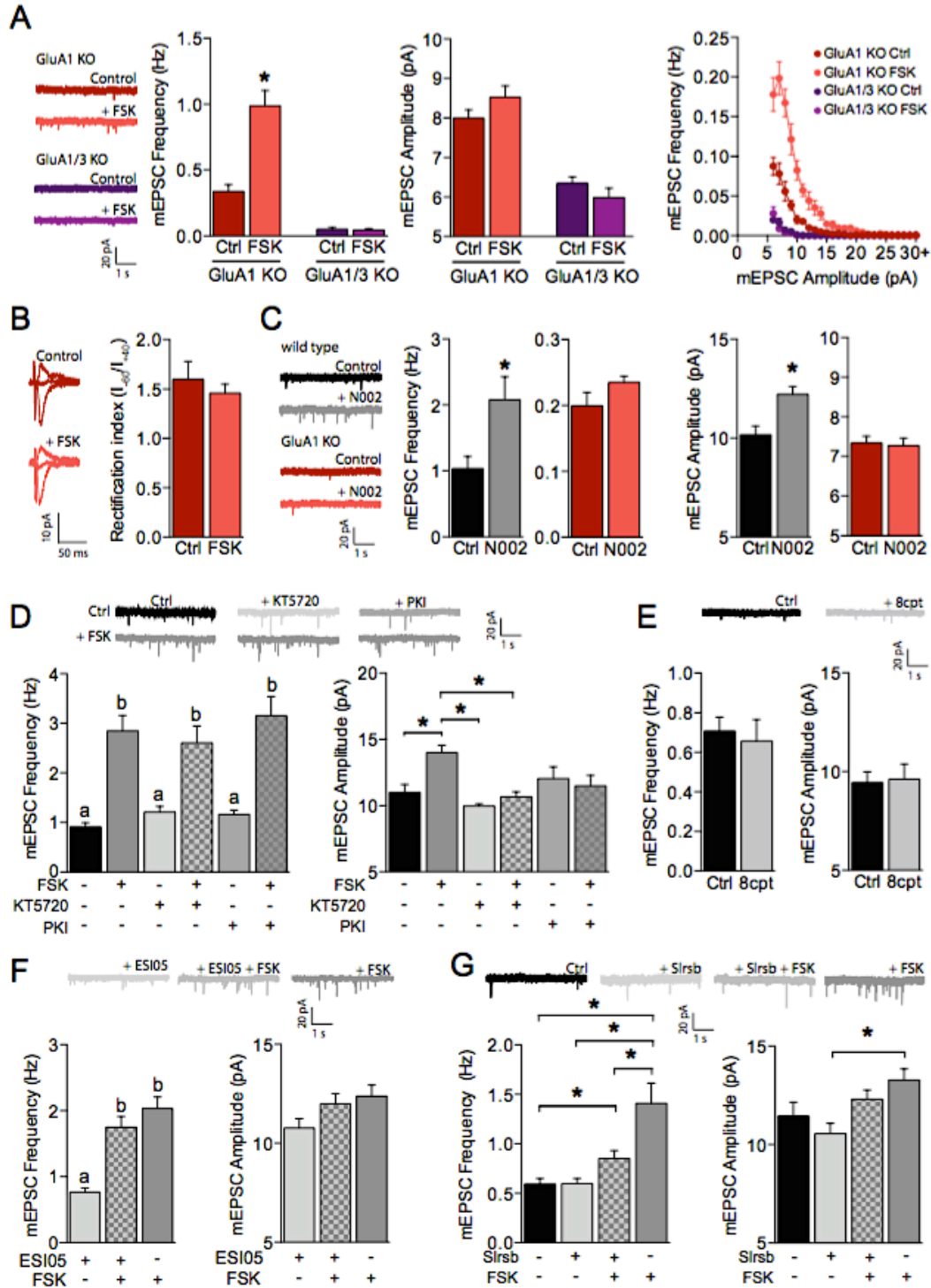


Figure 4. cAMP activates GluA2/3s via a PKA and Epac independent mechanism

(A) Example traces, mEPSC frequencies, mEPSC amplitudes of and mEPSC distribution per 1 pA binned amplitude of GluA1-KO neurons without (dark red; n=11) or with (light red; n=10) forskolin and GluA1/3-KO neurons without (dark purple; n=11) or with (light purple; n=8) forskolin. (B) GluA3 exists as GluA2/3 heteromeric AMPARs. Average rectification indices ($(I_{-60\text{mV}} - I_{0\text{mV}}) / (I_{+40\text{mV}} - I_{0\text{mV}})$) were determined in GluA1-KO organotypic slices of CA1 neurons without (n=6) or with (n=6) forskolin treatment. (C-F) PKA or Epac did not mediate GluA3-plasticity. (C) Example traces, mEPSC frequencies and mEPSC amplitudes of WT neurons with (n=12) or without (n=13) PKA agonist N002, and GluA1-KO neurons with (n=13) or without (n=15) N002 in the recording pipette. (D) Example traces, mEPSC frequencies and mEPSC amplitudes of untreated CA1 neurons (n=15), neurons incubated with forskolin (n=15), with PKA inhibitor KT5720 (n=10), preincubated with KT5720 prior to forskolin (n=10), incubated with PKA inhibitor PKI (n=7), or preincubated with PKI prior to forskolin (n=6). Different letters (a,b) indicate significant differences ($p < 0.05$). (E) Average mEPSC frequencies and amplitudes of CA1 neurons with control intracellular solution (n=7) or with Epac activator 8-CPT-2Me-cAMP in the recording pipette (n=7). (F) Same as (D) for CA1 neurons incubated with Epac inhibitor ESI-05 (n=12), forskolin (n=10) or preincubated with ESI-05 prior to forskolin (n=15). (G) Farnesyltransferase inhibitor Salirasib prevents GluA3-plasticity. Example traces, mEPSC frequencies and mEPSC amplitudes of untreated CA1 neurons (n=23), neurons incubated with forskolin (n=14), with Salirasib (n=18), preincubated with salirasib prior to forskolin (n=22). Error bars indicate SEM, * indicates $p < 0.05$.

frequency and amplitude in wild-type CA1 neurons ($p = 0.004$; Figure 4C). However, N002 did not increase the frequency or amplitude of mEPSC events in GluA1-deficient CA1 neurons ($p = 0.07$; Figure 4C). Moreover, pre-incubation of wild-type CA1 neurons with drugs that block PKA activation, KT5720 or PKI, failed to prevent the forskolin-mediated increase in mEPSC frequency (for both drugs $p > 0.9$; Figure 4D). KT 5720 was able to block the forskolin-driven increase in mEPSC amplitude, which may reflect a blockade of GluA1-trafficking. These data indicate that GluA3-plasticity is not mediated by PKA. We further excluded the involvement of the cAMP-dependent activation of HCN channels, since these channels were blocked by intracellular cesium during whole-cell recordings. We also found no evidence supporting a direct activation of GluA3 by cAMP (Figure S2B).

As an alternative cAMP pathway, the Epac family of the cAMP-regulated guanylyl exchange factors (GEFs) has been described (Gloerich and Bos 2010). A drug (ESI05) that inhibits Epac was unable to block the effect of forskolin ($p = 0.4$; Figure 4F), and adding the Epac activator 8-CPT-2Me-cAMP (8CPT) to the recording pipette did not increase the frequency of mEPSC events ($p = 0.5$; Figure 4E). These data suggest that GluA3-plasticity in CA1 neurons does not involve Epac, which is in line with previous findings that Epac activation does not increase synaptic currents in hippocampal neurons (Gelinas et al., 2008; Ster et al., 2009). Interestingly, in Chapter 3 we describe that cAMP-driven GluA3-plasticity is also operational in cerebellar Purkinje cells and, using the same experimental conditions as we used

here, we found that in these neurons GluA3-dependent synaptic potentiation is mediated by Epac (Gutierrez-Castellanos et al). Since signaling pathways tend to be conserved between different cell types, one could speculate that GluA3-plasticity in the hippocampus is mediated by a cAMP-regulated GEF that is homologous to Epac but insensitive to currently available Epac-selective drugs. GEFs activate GTPases including the superfamily of Ras-like proteins. To test the possibility that a member of the Ras superfamily is involved in mediating GluA3-plasticity, we tested an inhibitor of farnesyltransferases (FTs) of which Ras proteins are a substrate. The FT-inhibitor (Salirasib) significantly reduced the forskolin-mediated increase in mEPSC frequency ($p=0.04$, Figure 4G), indicating that GluA3-plasticity involves a mediator that depends on FT activity. We propose that a rise in cAMP can induce synaptic potentiation in CA1 neurons through two divergent signaling pathways: the trafficking of GluA1-containing AMPARs to the cell surface by PKA and the increase in the open-probability of GluA2/3s by a to-date unidentified cAMP-dependent GEF of Ras-like proteins.

NE-release triggers the activation of GluA3-plasticity

β -adrenergic receptor (β -AR) activation leads to an increase in intracellular cAMP levels (Seeds and Gilman, 1971). To assess whether β -AR activation can trigger GluA3-plasticity, we performed a mEPSC analysis on CA1 excitatory neurons of the dorsal hippocampus in brain slices acutely isolated from mature mice. The mEPSC frequency and amplitude were similar in CA1 neurons from wild-type and GluA3-deficient mice, suggesting that GluA3-containing AMPARs in CA1 neurons are in an inactive state under basal conditions. When these slices were incubated with the β -AR agonist isoproterenol we observed an increase in mEPSC frequency in CA1 neurons of wild-type mice, provided that cAMP degradation was inhibited with IBMX ($p<0.0001$; Figure 5A). Isoproterenol did not trigger synaptic potentiation in CA1 neurons of GluA3-deficient littermates ($p=0.6$; Figure 5A), indicating that β -AR activation is sufficient to evoke GluA3-plasticity when PDE activity is low.

To examine whether GluA3-plasticity can be induced *in vivo* through NE release, epinephrine (E) or saline as a control was injected intraperitoneally in mature mice. E stimulates the locus coeruleus (LC) to supply NE throughout the nervous system including the hippocampus, which enhances arousal and reduces the exploratory locomotor activity in rodents (Carter et al., 2010; Liang et al., 1986). When mice were placed in a novel environment 10 minutes after E-injection, both wild-type ($p=0.01$) and GluA3-deficient littermates ($p=0.03$) showed decreased locomotion to a similar

extent ($p=0.9$) (Figure 5B), suggesting that LC-activity is intact in GluA3-deficient mice. In brain slices prepared 10 minutes after E-injection we observed a significant increase in mEPSC frequency in the majority of CA1 neurons of wild-type mice ($p=0.002$), but not in neurons of GluA3-deficient mice ($p=0.8$; Figure 5C and S3A).

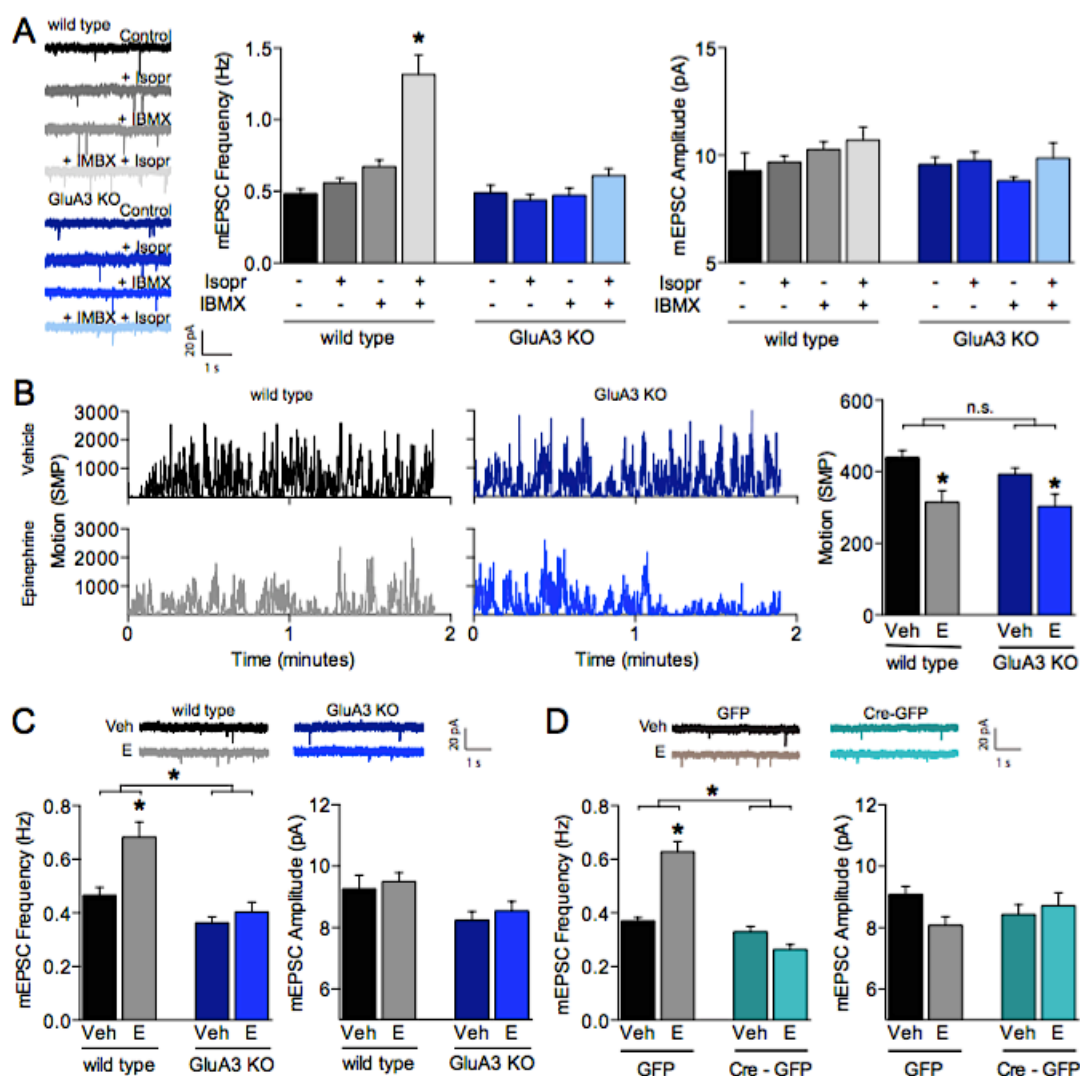


Figure 5. NE release triggers the activation of synaptic GluA3

(A) β -AR activation induces GluA3-plasticity. Brain slices were acutely isolated from mature WT and littermate GluA3-KO mice. Example traces, average mEPSC frequencies and amplitudes from CA1 neurons incubated with no drugs, β -AR agonist isoproterenol, PDE blocker IBMX, or isoproterenol plus IBMX (WT: Ctrl $n=13$, Iso $n=11$, IBMX $n=7$, Iso+IBMX $n=9$; GluA3-KO: Ctrl $n=15$, Iso $n=7$, IBMX $n=7$, Iso+IBMX $n=6$). (B) Epinephrine injection decreases the motion of both WT and GluA3-KO mice. Example traces and average motion as a change in significant motion pixels (SMPs) (Kopec et al., 2007) of WT injected with saline ($n=15$) or epinephrine ($n=15$) and GluA3-KO injected with saline ($n=17$) or E ($n=15$). (C) Example traces, mEPSC frequencies and mEPSC amplitudes of CA1 hippocampal neurons from WT mice injected with epinephrine ($n=15$) or saline ($n=13$) or GluA3-KO mice injected with epinephrine ($n=13$) or saline ($n=16$). (D) AAV virus expressing GFP or GFP-Cre were stereotactically targeted at the CA1 of fGluA3 mice. Example traces, mEPSC frequencies and mEPSC amplitudes recorded from GFP-positive CA1 neurons after injection

with epinephrine (GFP: n=11; GFP-Cre: n=9) or saline (GFP: n=11; GFP-Cre: n=11). Error bars indicate SEM, * indicates $p < 0.05$.

To assess whether synaptic potentiation upon E-injection required GluA3 in CA1 neurons, we repeated this experiment in mice that lacked GluA3 expression selectively in a subset of CA1 neurons. Three-week-old mice, whose GluA3 gene was flanked by loxP sites (fGluA3), were stereotactically injected with AAV5 virus expressing either Cre-GFP or GFP under control of the Synapsin promoter in the CA1 region of the hippocampus. After allowing Cre-recombinase to reduce GluA3 levels for three weeks, we injected E or saline intraperitoneally and measured mEPSCs on GFP-positive neurons from slices prepared 10 minutes after injection. Whereas the synaptic effect of E injection was evident in slices prepared from mice injected with control GFP-virus ($p < 0.0001$), it was abolished in neurons where GluA3 expression had been knocked out by Cre-recombinase ($p = 0.06$; Figure 5D). These data indicate that E-injection is sufficient to induce GluA3-plasticity in CA1 pyramidal neurons.

GluA3-plasticity is induced by fear but does not contribute to memory formation

Mice were allowed to explore a novel environment whereupon they received three electric shocks (0.8 mA) as an aversive stimulus. In wild-type mice this fear conditioning protocol led to the formation of contextual fear memories that remained stable over time (Figure 6A,B,E). Fear induced in mice by foot shocks in an unfamiliar context triggers the acute release of NE in the hippocampus, which peaks approximately 10 minutes after delivery of the shocks (Bremner et al., 1996; McIntyre et al., 2002). To assess whether such fear elicits synaptic plasticity in the CA1 region of the hippocampus, brain slices were prepared 10 minutes after fear conditioning and mEPSCs were recorded from pyramidal neurons. A significant increase in the frequency of mEPSC events was observed ($p < 0.0001$; Figure 6C) in the majority of CA1 pyramidal neurons (Figure S3B), which was not accompanied by changes in average mEPSC amplitude ($p = 0.6$; Figure 6C), spine density or average spine size at apical dendrites (Figure S4A). When wild-type mice were injected with β -AR antagonist propranolol 30 minutes prior to fear conditioning, the increase in mEPSC frequency in slices prepared 10 minutes after administering foot shocks was significantly reduced compared to saline-injected control mice ($p = 0.02$; Figure 6D),

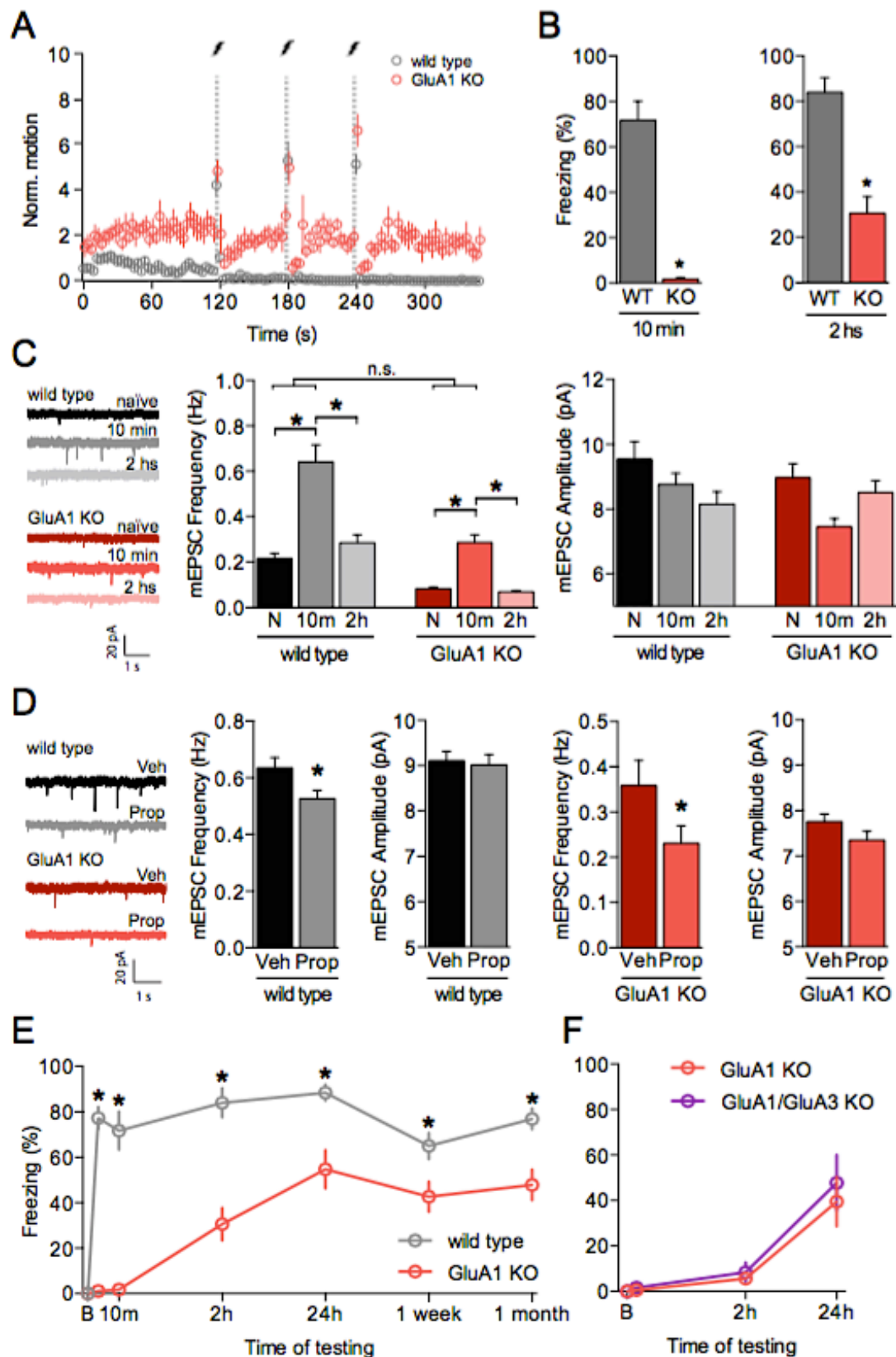


Figure 6. Fear triggers a GluA1-independent synaptic potentiation in CA1 neurons

Mice received a fear conditioning session consisting of three electric shocks of 0.80mA (A-F). (A) Locomotion was quantified during fear conditioning in WT (n=17) and GluA1-KO (n=16)

littermates. (B) Freezing levels when re-exposed to the shock cage either 10 min (WT: n=8; GluA1-KO: n=8) or 2 hours (WT: n=9; GluA1-KO: n=8) after conditioning. (C) Slices were prepared from naïve mice or from mice 10 min or 2 hours after conditioning of WT (N: n=29 neurons, 10m: n=12, 2h: n=21) or GluA1-KO mice (N: n=29, 10m: n=19, 2h: n=30) littermates. (D) WT and GluA1-KO mice were injected with propranolol 30 min prior to fear conditioning and brain slices were prepared 10 min after conditioning. Example traces, mEPSC frequencies and amplitudes were recorded from WT (Ctrl: n=22, Prop: n=16) and GluA1-KO (Ctrl: n=10, Prop: n=9) CA1 neurons. (E) Whereas contextual fear memories of WT mice are stable in time, in GluA1-KO mice the expression of fear memories gradually increases in time. Different groups of WT (10 min: n=8; 2hrs: n=9; 24hrs: n=8; 1 week: n=12; 1 month: n=5) and GluA1-KO (10 min: n=8; 2hrs: n=8; 24hrs: n=7; 1 week: n=12; 1 month: n=10) littermate mice were re-exposed to the shock cage and freezing levels were quantified. (E) Both GluA1-KO and GluA1/GluA3 double KO littermates display gradually increasing fear memories. Different groups of GluA1-KO (2hrs: n=7; 24hrs: n=9) and GluA1/3-KO (2hrs: n=6; 24hrs: n=8) littermates were re-exposed to the shock cage and freezing levels were quantified.

indicating that fear-induced plasticity relies at least in part on β -AR activation. The synaptic potentiation of CA1 neurons elicited by the fearful experience was transient: in acute slices prepared 2 hours after fear conditioning mEPSC frequency had returned to baseline levels (Figure 6C). These results are consistent with previous observations that contextual fear conditioning is accompanied by a change in synaptic strength in the CA1 region of the hippocampus (Zhou et al. 2009; Whitlock et al. 2006).

Fear conditioning leads to the activation of GluA1-dependent plasticity in a proportion of CA1 hippocampal neurons (Mitsushima et al. 2011). To study whether fear also triggers GluA1-independent forms of synaptic plasticity, GluA1-deficient mice were fear conditioned and their memory was assessed. In contrast to wild-type littermates, GluA1-deficient mice did not show any freezing response immediately following the shocks ($p < 0.0001$; Figure 6A) or following re-exposure to the shock-cage 10 minutes after conditioning ($p < 0.0001$; Figure 6B). Despite these differences, fear conditioning did induce a transient increase in mEPSC frequency in the majority of CA1 neurons in slices from GluA1-deficient mice ($p < 0.0001$, Figure 6C and S3B). This increase, which required β -AR activation ($p = 0.04$; Figure 6D), was smaller in absolute size compared with that in slices from wild-type littermates ($p < 0.0001$), but similar in relative magnitude ($p = 0.7$). These experiments suggest that synaptic plasticity was induced in the absence of GluA1 through the activation of β -ARs shortly after a fearful event. Interestingly, GluA1-deficient mice were able to gradually develop long-term contextual fear memories. Although they never reached the freezing levels of wild-type littermates ($p = 0.03$; Figure 6E), they did freeze significantly when re-

exposed to the shock-cage at later time points (10 min vs. 1 month: $p < 0.001$). Note that each group of mice was tested only once to avoid effects of extinction or habituation in the fear response (see methods). A similar time-course of slowly developing fear responses was observed in mice that lack both GluA1 and GluA3 (Figure 6F), indicating that these delayed memories relied on plasticity mechanisms that did not involve GluA1 or GluA3.

The behavior of GluA3-deficient mice during the fear conditioning protocol was normal: their locomotor activity was similar to wild-type littermates when put in a novel environment ($p = 0.9$) and their startle response to the shocks did not differ ($p = 0.8$, Figure 7A). GluA3-deficient mice showed freezing levels similar to those of wild-type littermates when re-exposed to the shock-cage either 10 minutes ($p > 0.9$) or 2 hours ($p = 0.4$) after fear conditioning (Figure 7B). To examine whether fear conditioning induced GluA3-plasticity in the hippocampus, we recorded mEPSCs in brain slices isolated from GluA3-deficient and wild-type littermates. In CA1 neurons of GluA3-deficient mice an increase in mEPSC frequency was observed in slices isolated 10 minutes after fear conditioning ($p = 0.0004$; Figure 7C), likely as a consequence of GluA1-plasticity and/or presynaptic plasticity. Importantly, this increase in mEPSC frequency was substantially smaller in magnitude than that in CA1 neurons of wild-type littermates ($p = 0.005$), indicating that GluA3-plasticity was induced in the CA1 region of the hippocampus of wild-type mice. Similarly, when GluA3 was knocked out by Cre-expression selectively in the CA1 region of fGluA3 mice after development, the increase in mEPSC frequency from Cre-positive cells of slices isolated 10 minutes after fear conditioning was significantly smaller compared with neurons expressing GFP as a control ($p = 0.001$; Figure 7D). These experiments indicate that GluA3-plasticity is induced in CA1 pyramidal neurons by the fear conditioning experience. GluA3-plasticity did not contribute to the formation or stability of fear memories; if anything, long-term memories tended to be slightly improved in GluA3-deficient mice compared to wild-type littermates (Figure 7E). The fear responses were equally context-specific for wild-type and GluA3-deficient mice ($p = 0.6$; Figure 7F), indicating that the absence of GluA3 did not cause a generalization of conditioned fear. Moreover, GluA3 did not play a role in a more protracted type of learning: the reward-based two-choice discrimination task was unaffected (WT vs GluA3-KO: $p > 0.9$; Figure S5A,B). These data indicate that in contrast to GluA1-dependent plasticity, GluA3-plasticity does not directly contribute to hippocampal learning, underscoring the functional relevance of AMPAR-subunit composition.

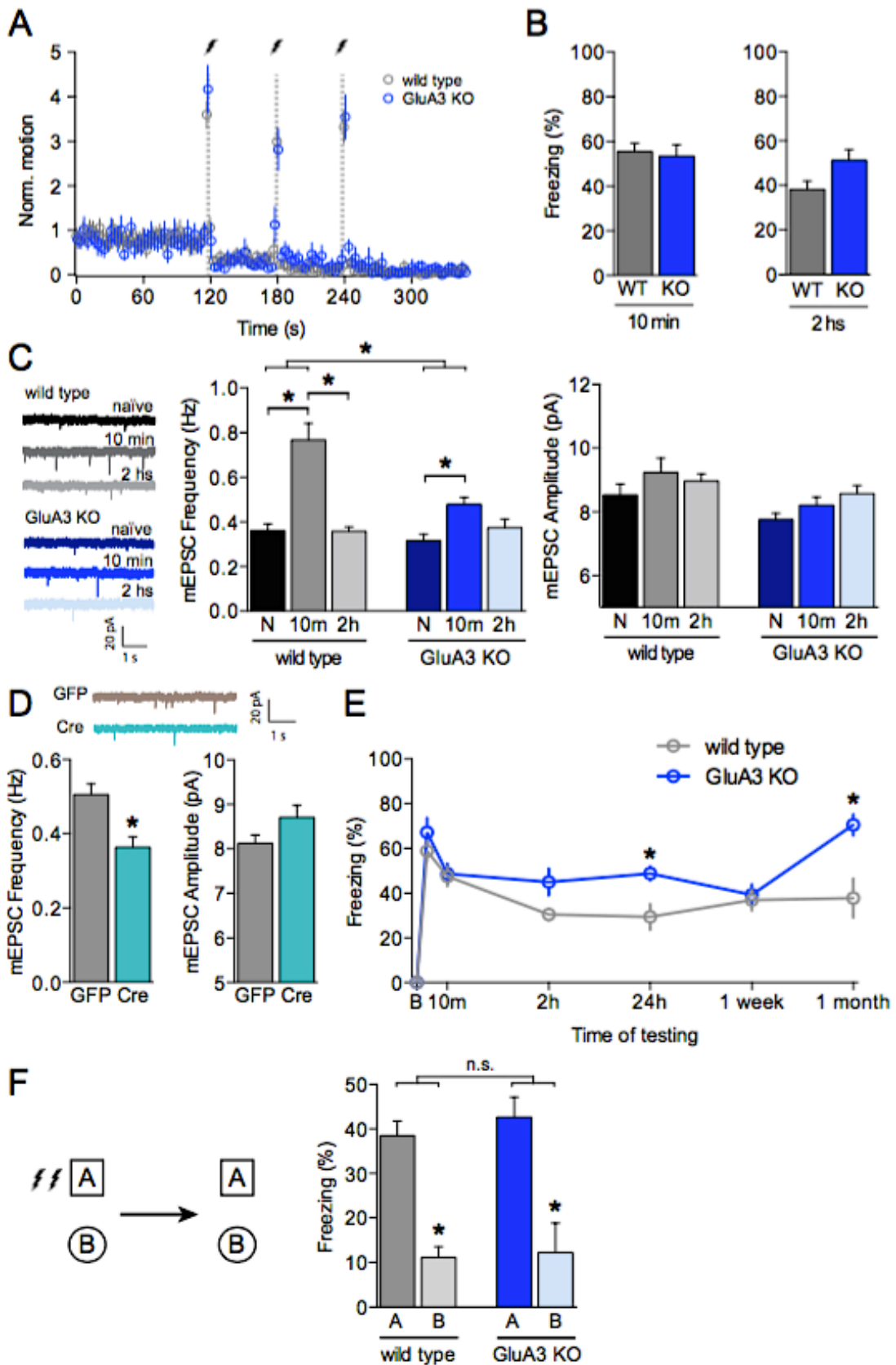


Figure 7. Fear triggers a GluA3-plasticity in CA1 neurons

Mice received a fear conditioning session consisting of three electric shocks of 0.80mA (A-D,F) or 0.65mA (E). (A) Locomotion was quantified during fear conditioning in WT (n=22) and GluA3-KO (n=22) littermates. (B) Freezing levels when re-exposed to the shock cage either

10 min (WT: n=11; GluA3-KO: n=11) or 2 hours (WT: n=11; GluA3-KO: n=11) after conditioning. (C) Slices were prepared from naïve mice or from mice 10 min or 2 hours after conditioning of WT (N: n=15, 10m: n=18, 2h: n=16) or GluA3-KO mice (N: n=22, 10m: n=22, 2h: n=10) littermates. (D) flGluA3 mice stereotactically injected as in Figure 5D were subjected to fear conditioning, and 10 min later brain slices were prepared. Example traces, average mEPSC frequencies and amplitudes of Cre-GFP (n=11) and control GFP (n=15). (E) Contextual fear memories of both WT and GluA3-KO mice are stable in time. Different groups of WT (10 min: n=11; 2hrs: n=11; 24hrs: n=10; 1 week: n=10; 1 month: n=5) and GluA3-KO (10 min: n=11; 2hrs: n=11; 24hrs: n=8; 1 week: n=6; 1 month: n=7) littermates were re-exposed to the shock cage and freezing levels were quantified. (F) Fear memories in WT and GluA3-KO mice are context specific. WT (n=13) and GluA3-KO (n=12) are exposed to context A and context B but only receive shocks in A. 2 Hours later they are re-exposed to both context A and B and freezing levels are scored.

DISCUSSION

In this study we identified a form of synaptic plasticity in the CA1 region of the hippocampus that depends on GluA3-containing AMPARs. Historically, AMPARs of hippocampal neurons have been assumed to predominantly consist of GluA1/2s with only a small proportion of GluA2/3s. This notion was based on the observations that mRNA levels of GluA3 are 10-fold lower compared with GluA1 and GluA2 mRNA levels (Tsuzuki et al., 2001) and that GluA2/3s contribute little to synaptic and extrasynaptic AMPAR currents (Andrásfalvy et al., 2003; Lu et al., 2009). However, the total protein levels of GluA3 in the hippocampus were shown to be substantial (Schwenk et al., 2014), and it was estimated that the AMPAR population in CA1 dendrites is composed of equivalent amounts of GluA1/2s and GluA2/3s (Kessels et al., 2009). We here unify these seemingly contradictory findings by showing that GluA3-containing AMPARs are present at synapses and on the cell surface; however, they are electrically quiet under basal conditions.

GluA3-mediated currents become visible when intracellular cAMP levels are increased in CA1 neurons. Our single-channel recordings indicate that these increased currents are a consequence of an improved capacity of glutamate to open the AMPAR channel. GluA1-containing AMPARs opened their channels independently of cAMP levels, suggesting that this type of AMPAR channel plasticity is an exclusive feature of GluA3. Future structural studies may reveal whether cAMP triggers a putative conformational change within the GluA3 subunit that allows either glutamate to access the ligand binding site or glutamate binding to open the channel. The activation of GluA3-plasticity by cAMP is fast, since outside-out patches were pulled from whole-cell configuration after allowing cAMP to flow inside the cell for ~10 seconds. It remains to be established which intermediate player induces the cAMP activation responsible for the increased currents mediated by GluA2/3s. We did not find evidence for cAMP to act via its known neuronal targets (PKA, HCN channels, Epac) or directly onto GluA3. Based on our findings that GluA3-plasticity in cerebellar Purkinje cells is mediated by Epac, the cAMP-regulated GEF for Rap1 (see Chapter 3), and that GluA3-plasticity in CA1 neurons is reduced by a FT inhibitor, which is known to block the activity of Ras-like proteins, we consider the possibility that GluA3-plasticity in the hippocampus is mediated by a to-date unidentified cAMP-regulated GEF for a member of the Ras-superfamily.

The cAMP-driven activation of surface GluA2/3s mirrors GluA3-plasticity at synapses: both increased approximately two-fold in currents upon a rise in cAMP.

These results imply that similar to its total levels at CA1 dendrites (Kessels et al., 2009) approximately half of the synaptic and extrasynaptic AMPAR population consists of GluA2/3s. When recombinant GluA3 was expressed in GluA3-deficient CA1 neurons of organotypic slices, the newly formed GluA3-containing AMPARs did not cause a change in synaptic or extrasynaptic AMPAR currents. However, upon a rise in cAMP they showed increased currents at both synaptic and extrasynaptic sites without a change in GluA3 surface levels. These findings suggest that GluA2/3s had trafficked to the cell surface and into synapses in the absence of LTP-like activity. Similarly, the activation of GluA3-plasticity upon fear conditioning was not accompanied by a change in spine size or spine number (Figure S4A). Considering that the number of AMPARs at CA1 synapses correlates well with spine size (Matsuzaki et al., 2001), GluA3s may have been already present at synapses before learning. Our results are therefore in line with the AMPAR subunit-specific rules for synaptic plasticity: unlike GluA1-containing AMPARs, GluA3-containing AMPARs do not require LTP-like activity to traffic onto the cell surface and into synapses (Kessels et al., 2009; Makino and Malinow, 2009; Shi et al., 2001). A recent study showed that in the absence of GluA1, GluA1-lacking AMPARs can be added to synapses upon the induction of LTP (Granger et al., 2013). Although this study did not show whether this is also the case for GluA2/3s, our finding that GluA2/3s are electrically quiet under basal conditions may explain why LTP is not visible in GluA1-deficient hippocampal slices (Granger et al., 2013; Zamanillo et al., 1999). Previous studies showed that a slowly arising LTP can be seen in GluA1-deficient slices when a theta-burst stimulation is paired with a postsynaptic depolarization (Frey et al., 2009). We speculate that upon this stimulation protocol a gradual increase in cAMP levels may have activated GluA3-plasticity.

Whereas GluA3 is uniformly distributed within synapses, GluA1 tends to be more concentrated towards their edges (Jacob and Weinberg, 2015) and large CA1 synapses are particularly enriched in GluA1 (Shinohara & Hirase 2009). This notion that GluA1/2s and GluA2/3s are differentially distributed at CA1 synapses may explain why the postsynaptic activation of GluA3-containing AMPARs was largely reflected as an increase in mEPSC frequency without necessarily a change in average mEPSC amplitude. A large proportion of mEPSCs recorded from CA1 neurons fell below the 5 pA detection limit (Figure 3C, 4A). When a mEPSC is generated by the release of a single vesicle onto a micro-domain within a synapse that predominantly contains GluA2/3s (MacGillavry et al., 2013), its amplitude may only overpass the detection limit after a rise in cAMP. Reversely, glutamate binding

to a micro-domain that contains mainly GluA1 and little GluA3 may produce mEPSCs that are detectable under basal conditions, but the amplitude of such mEPSCs will benefit only little from GluA3-plasticity. In such a scenario, the frequency of mEPSC events increases more than their average amplitude. Similarly, CA1 neurons, in which either GluA1 or GluA3 are depleted, are mostly affected in mEPSC frequency and little in amplitude (Lu et al., 2009). We therefore propose that variations in mEPSC frequency, if not caused by a change in presynaptic vesicle release or the number of functional synapses, may be a manifestation of a postsynaptic AMPAR subunit-specific effect.

Our experiments indicate that the activation of β -ARs can stimulate two independent forms of AMPAR plasticity in parallel. First, PKA phosphorylation of GluA1-containing AMPARs facilitates their trafficking to synapses (Man et al., 2007), thereby facilitating memory formation (Hu et al., 2007). We identified a second cAMP-dependent form of AMPAR plasticity. Our data show that GluA2/3-dependent currents are increased by β -AR activation following a fearful experience. Other signaling pathways that lead to a rise in intracellular cAMP, like for instance those activated by dopamine or serotonin release, may theoretically also lead to the activation of GluA3-plasticity. Besides the hippocampus, GluA3-containing AMPARs are present in most other brain regions, including the cortex, amygdala, striatum, thalamus, brain stem, olfactory bulb, nucleus accumbens and cerebellum (Breese et al., 1996; Reimers et al., 2011; Schwenk et al., 2014), suggesting that GluA3-plasticity may be operative throughout the brain. In Chapter 3 we demonstrate that Purkinje cells of the cerebellum also express both GluA1- and GluA3-containing AMPARs, but in these neurons GluA3, and not GluA1, was crucial for synaptic strengthening and motor learning (Gutierrez-Castellanos et al.). Thus, the AMPAR subunit rules for synaptic plasticity are inverted in Purkinje neurons with respect to those in CA1 hippocampal neurons.

Fear learning depends on GluA1-dependent long-term potentiation of a subset of synapses on a fraction of neurons in the hippocampus and the lateral amygdala (Mitsushima et al., 2011; Rumpel et al., 2005). We show that fear also induced a GluA3-dependent form of short-term synaptic potentiation in the majority of CA1 neurons. When considering that fear memories require sparse coding and remain present long-term, it may not be surprising that GluA3-plasticity does not contribute to hippocampus-dependent memory formation. GluA3-plasticity also did not mask a memory by selectively potentiating synapses that took no part in the memory engram, since GluA3-deficient mice displayed fear responses indistinguishable from

wild-type littermates shortly after fear conditioning when GluA3s are largely active. It was previously suggested that GluA2/3s gradually replace GluA1-containing AMPARs at synapses after experience-dependent plasticity (McCormack et al., 2006; Takahashi et al., 2003). This AMPAR-subunit replacement process does not appear to be necessary to stabilize a memory, since we observed that fear memories remained stable in GluA3-deficient mice for up to one month after fear conditioning. In theory, the replacement of GluA1- for GluA3-containing AMPARs may have an adverse effect on the preservation of memories as GluA3 channels would be partly inactive after replacement. Perhaps this explains why in some instances we observed stronger long-term memories in GluA3-deficient mice compared to wild-type littermates. Interestingly, GluA3-plasticity is likely a selective feature of excitatory neurons, since most inhibitory neurons in the hippocampus lack GluA2/3s (Leranth et al., 1996). The activation of GluA3-plasticity may therefore selectively promote excitation, potentially enhancing information transfer during an emotional experience. The previous observation that GluA3-deficient mice display more aggressive behavior (Adamczyk et al., 2012) may be in line with a possible role of GluA3-plasticity in the control of emotional behavior.

REFERENCES

- Adamczyk, A., Mejias, R., Takamiya, K., Yocum, J., Krasnova, I.N., Calderon, J., Cadet, J.L., Haganir, R.L., Pletnikov, M. V, and Wang, T. (2012). GluA3-deficiency in mice is associated with increased social and aggressive behavior and elevated dopamine in striatum. *Behav. Brain Res.* 229, 265–272.
- Alvarez, O., Gonzalez, C., and Latorre, R. (2002). Counting channels: a tutorial guide on ion channel fluctuation analysis. *Adv. Physiol. Educ.* 26, 327–341.
- Andrásfalvy, B.K., Smith, M.A., Borchardt, T., Sprengel, R., and Magee, J.C. (2003). Impaired regulation of synaptic strength in hippocampal neurons from GluR1-deficient mice. *J. Physiol.* 552, 35–45.
- Bernard, V., Somogyi, P., and Bolam, J.P. (1997). Cellular, subcellular, and subsynaptic distribution of AMPA-type glutamate receptor subunits in the neostriatum of the rat. *J. Neurosci.* 17, 819–833.
- Breese, C.R., Logel, J., Adams, C., and Leonard, S.S. (1996). Regional gene expression of the glutamate receptor subtypes GluR1, GluR2, and GluR3 in human postmortem brain. *J. Mol. Neurosci.* 7, 277–289.
- Bremner, J.D., Krystal, J.H., Southwick, S.M., and Charney, D.S. (1996). Noradrenergic mechanisms in stress and anxiety: I. Preclinical studies. *Synapse* 23, 28–38.
- Carroll, R.C., Nicoll, R.A., and Malenka, R.C. (1998). Effects of PKA and PKC on miniature excitatory postsynaptic currents in CA1 pyramidal cells. *J. Neurophysiol.* 80, 2797–2800.
- Carter, M.E., Yizhar, O., Chikahisa, S., Nguyen, H., Adamantidis, A., Nishino, S., Deisseroth, K., and de Lecea, L. (2010). Tuning arousal with optogenetic modulation of locus coeruleus neurons. *Nat. Neurosci.* 13, 1526–1533.
- Chavez-Noriega, L.E., and Stevens, C.F. (1992). Modulation of synaptic efficacy in field CA1 of the rat hippocampus by forskolin. *Brain Res.* 574, 85–92.
- Crombag, H.S., Sutton, J.M., Takamiya, K., Lee, H.-K., Holland, P.C., Gallagher, M., and Haganir, R.L. (2008). A necessary role for GluR1 serine 831 phosphorylation in appetitive incentive learning. *Behav. Brain Res.* 191, 178–183.
- Frey, M.C., Sprengel, R., and Nevian, T. (2009). Activity pattern-dependent long-term potentiation in neocortex and hippocampus of GluA1 (GluR-A) subunit-deficient mice. *J. Neurosci.* 29, 5587–5596.
- Gelinas, J.N., Banko, J.L., Peters, M.M., Klann, E., Weeber, E.J., and Nguyen, P. V (2008). Activation of exchange protein activated by cyclic-AMP enhances long-lasting synaptic potentiation in the hippocampus. *Learn. Mem.* 15, 403–411.
- Gloerich, M., and Bos, J.L. (2010). Epac: defining a new mechanism for cAMP action. *Annu. Rev. Pharmacol. Toxicol.* 50, 355–375.
- Granger, A.J., Shi, Y., Lu, W., Cerpas, M., and Nicoll, R.A. (2013). LTP requires a reserve pool of glutamate receptors independent of subunit type. *Nature* 493, 495–500.

- Hall, R.A. (2004). Beta-adrenergic receptors and their interacting proteins. *Semin. Cell Dev. Biol.* 15, 281–288.
- Hartveit, E., and Veruki, M.L. (2007). Studying properties of neurotransmitter receptors by non-stationary noise analysis of spontaneous postsynaptic currents and agonist-evoked responses in outside-out patches. *Nat. Protoc.* 2, 434–448.
- Hu, H., Real, E., Takamiya, K., Kang, M.-G., Ledoux, J., Hugarir, R.L., and Malinow, R. (2007). Emotion enhances learning via norepinephrine regulation of AMPA-receptor trafficking. *Cell* 131, 160–173.
- Hugarir, R.L., and Nicoll, R.A. (2013). AMPARs and synaptic plasticity: the last 25 years. *Neuron* 80, 704–717.
- Humeau, Y., Reisel, D., Johnson, A.W., Borchardt, T., Jensen, V., Gebhardt, C., Bosch, V., Gass, P., Bannerman, D.M., Good, M.A., et al. (2007). A pathway-specific function for different AMPA receptor subunits in amygdala long-term potentiation and fear conditioning. *J. Neurosci.* 27, 10947–10956.
- Jacob, A.L., and Weinberg, R.J. (2015). The organization of AMPA receptor subunits at the postsynaptic membrane. *Hippocampus* 25, 798–812.
- Joiner, M.A., Lisé, M.-F., Yuen, E.Y., Kam, A.Y.F., Zhang, M., Hall, D.D., Malik, Z.A., Qian, H., Chen, Y., Ulrich, J.D., et al. (2010). Assembly of a beta2-adrenergic receptor--GluR1 signalling complex for localized cAMP signalling. *EMBO J.* 29, 482–495.
- Kerchner, G.A., and Nicoll, R.A. (2008). Silent synapses and the emergence of a postsynaptic mechanism for LTP. *Nat. Rev. Neurosci.* 9, 813–825.
- Kessels, H.W., and Malinow, R. (2009). Synaptic AMPA receptor plasticity and behavior. *Neuron* 61, 340–350.
- Kessels, H.W., Kopec, C.D., Klein, M.E., and Malinow, R. (2009). Roles of stargazin and phosphorylation in the control of AMPA receptor subcellular distribution. *Nat. Neurosci.* 12, 888–896.
- Kharazia, V.N., and Weinberg, R.J. (1997). Tangential synaptic distribution of NMDA and AMPA receptors in rat neocortex. *Neurosci. Lett.* 238, 41–44.
- Kim, C.-H., Takamiya, K., Petralia, R.S., Sattler, R., Yu, S., Zhou, W., Kalb, R., Wenthold, R., and Hugarir, R. (2005). Persistent hippocampal CA1 LTP in mice lacking the C-terminal PDZ ligand of GluR1. *Nat. Neurosci.* 8, 985–987.
- Kopec, C.D., Kessels, H.W.H.G., Bush, D.E.A., Cain, C.K., LeDoux, J.E., and Malinow, R. (2007). A robust automated method to analyze rodent motion during fear conditioning. *Neuropharmacology* 52, 228–233.
- Lee, Y.-S., Ehninger, D., Zhou, M., Oh, J.-Y., Kang, M., Kwak, C., Ryu, H.-H., Butz, D., Araki, T., Cai, Y., et al. (2014). Mechanism and treatment for learning and memory deficits in mouse models of Noonan syndrome. *Nat. Neurosci.* 17, 1736–1743.
- Leranth, C., Szeideemann, Z., Hsu, M., and Buzsáki, G. (1996). AMPA receptors in the rat and primate hippocampus: a possible absence of GluR2/3 subunits in most interneurons. *Neuroscience* 70, 631–652.

- Liang, K.C., Juler, R.G., and McGaugh, J.L. (1986). Modulating effects of posttraining epinephrine on memory: involvement of the amygdala noradrenergic system. *Brain Res.* *368*, 125–133.
- Lu, W., Shi, Y., Jackson, A.C., Bjorgan, K., During, M.J., Sprengel, R., Seeburg, P.H., and Nicoll, R.A. (2009). Subunit composition of synaptic AMPA receptors revealed by a single-cell genetic approach. *Neuron* *62*, 254–268.
- MacGillavry, H.D., Song, Y., Raghavachari, S., and Blanpied, T.A. (2013). Nanoscale scaffolding domains within the postsynaptic density concentrate synaptic AMPA receptors. *Neuron* *78*, 615–622.
- Makino, H., and Malinow, R. (2009). AMPA receptor incorporation into synapses during LTP: the role of lateral movement and exocytosis. *Neuron* *64*, 381–390.
- Malinow, R., and Malenka, R.C. (2002). AMPA receptor trafficking and synaptic plasticity. *Annu. Rev. Neurosci.* *25*, 103–126.
- Man, H.-Y., Sekine-Aizawa, Y., and Huganir, R.L. (2007). Regulation of {alpha}-amino-3-hydroxy-5-methyl-4-isoxazolepropionic acid receptor trafficking through PKA phosphorylation of the Glu receptor 1 subunit. *Proc. Natl. Acad. Sci. U. S. A.* *104*, 3579–3584.
- Matsuzaki, M., Ellis-Davies, G.C., Nemoto, T., Miyashita, Y., Iino, M., and Kasai, H. (2001). Dendritic spine geometry is critical for AMPA receptor expression in hippocampal CA1 pyramidal neurons. *Nat. Neurosci.* *4*, 1086–1092.
- McCormack, S.G., Stornetta, R.L., and Zhu, J.J. (2006). Synaptic AMPA receptor exchange maintains bidirectional plasticity. *Neuron* *50*, 75–88.
- McIntyre, C.K., Hatfield, T., and McGaugh, J.L. (2002). Amygdala norepinephrine levels after training predict inhibitory avoidance retention performance in rats. *Eur. J. Neurosci.* *16*, 1223–1226.
- Meng, Y., Zhang, Y., and Jia, Z. (2003). Synaptic Transmission and Plasticity in the Absence of AMPA Glutamate Receptor GluR2 and GluR3. *Neuron* *39*, 163–176.
- Mitsushima, D., Ishihara, K., Sano, A., Kessels, H.W., and Takahashi, T. (2011). Contextual learning requires synaptic AMPA receptor delivery in the hippocampus. *Proc. Natl. Acad. Sci. U. S. A.* *108*, 12503–12508.
- Nabavi, S., Fox, R., Proulx, C.D., Lin, J.Y., Tsien, R.Y., and Malinow, R. (2014). Engineering a memory with LTD and LTP. *Nature* *511*, 348–352.
- Porrero, C., Rubio-Garrido, P., Avendaño, C., and Clascá, F. (2010). Mapping of fluorescent protein-expressing neurons and axon pathways in adult and developing Thy1-eYFP-H transgenic mice. *Brain Res.* *1345*, 59–72.
- Qian, H., Matt, L., Zhang, M., Nguyen, M., Patriarchi, T., Koval, O.M., Anderson, M.E., He, K., Lee, H.-K., and Hell, J.W. (2012). β 2-Adrenergic receptor supports prolonged theta tetanus-induced LTP. *J. Neurophysiol.* *107*, 2703–2712.
- Reimers, J.M., Milovanovic, M., and Wolf, M.E. (2011). Quantitative analysis of AMPA receptor subunit composition in addiction-related brain regions. *Brain Res.* *1367*, 223–233.
- Rumbaugh, G., Adams, J.P., Kim, J.H., and Huganir, R.L. (2006). SynGAP regulates

synaptic strength and mitogen-activated protein kinases in cultured neurons. *Proc. Natl. Acad. Sci. U. S. A.* *103*, 4344–4351.

Rumpel, S., LeDoux, J., Zador, A., and Malinow, R. (2005). Postsynaptic receptor trafficking underlying a form of associative learning. *Science* *308*, 83–88.

Sanchis-Segura, C., Borchardt, T., Vengeliene, V., Zghoul, T., Bachteler, D., Gass, P., Sprengel, R., and Spanagel, R. (2006). Involvement of the AMPA receptor GluR-C subunit in alcohol-seeking behavior and relapse. *J. Neurosci.* *26*, 1231–1238.

Schwenk, J., Baehrens, D., Haupt, A., Bildl, W., Boudkkazi, S., Roeper, J., Fakler, B., and Schulte, U. (2014). Regional Diversity and Developmental Dynamics of the AMPA-Receptor Proteome in the Mammalian Brain. *Neuron* *84*, 41–54.

Seeds, N.W., and Gilman, A.G. (1971). Norepinephrine stimulated increase of cyclic AMP levels in developing mouse brain cell cultures. *Science* *174*, 292.

Shi, S., Hayashi, Y., Esteban, J.A., and Malinow, R. (2001). Subunit-specific rules governing AMPA receptor trafficking to synapses in hippocampal pyramidal neurons. *Cell* *105*, 331–343.

Shinohara, Y., and Hirase, H. (2009). Size and Receptor Density of Glutamatergic Synapses: A Viewpoint from Left-Right Asymmetry of CA3-CA1 Connections. *Front. Neuroanat.* *3*, 10.

Sokolova, I. V., Lester, H.A., and Davidson, N. (2006). Postsynaptic mechanisms are essential for forskolin-induced potentiation of synaptic transmission. *J. Neurophysiol.* *95*, 2570–2579.

Ster, J., de Bock, F., Bertaso, F., Abitbol, K., Daniel, H., Bockaert, J., and Fagni, L. (2009). Epac mediates PACAP-dependent long-term depression in the hippocampus. *J. Physiol.* *587*, 101–113.

Stoppini, L., Buchs, P.A., and Muller, D. (1991). A simple method for organotypic cultures of nervous tissue. *J. Neurosci. Methods* *37*, 173–182.

Sukumaran, M., Rossmann, M., Shrivastava, I., Dutta, A., Bahar, I., and Greger, I.H. (2011). Dynamics and allosteric potential of the AMPA receptor N-terminal domain. *EMBO J.* *30*, 972–982.

Takahashi, T., Svoboda, K., and Malinow, R. (2003). Experience strengthening transmission by driving AMPA receptors into synapses. *Science* *299*, 1585–1588.

Tsuzuki, K., Lambolez, B., Rossier, J., and Ozawa, S. (2001). Absolute quantification of AMPA receptor subunit mRNAs in single hippocampal neurons. *J. Neurochem.* *77*, 1650–1659.

Vanhoose, A.M., and Winder, D.G. (2003). NMDA and beta1-adrenergic receptors differentially signal phosphorylation of glutamate receptor type 1 in area CA1 of hippocampus. *J. Neurosci.* *23*, 5827–5834.

Wenthold, R., Petralia, R., Blahos J, I., and Niedzielski, A. (1996). Evidence for multiple AMPA receptor complexes in hippocampal CA1/CA2 neurons. *J. Neurosci.* *16*, 1982–1989.

Whitlock, J.R., Heynen, A.J., Shuler, M.G., and Bear, M.F. (2006). Learning induces long-term potentiation in the hippocampus. *Science* *313*, 1093–1097.

Zamanillo, D., Sprengel, R., Hvalby, O., Jensen, V., Burnashev, N., Rozov, A., Kaiser, K.M., Köster, H.J., Borchardt, T., Worley, P., et al. (1999). Importance of AMPA receptors for hippocampal synaptic plasticity but not for spatial learning. *Science* *284*, 1805–1811.

Zhou, M., Conboy, L., Sandi, C., Joëls, M., and Krugers, H.J. (2009). Fear conditioning enhances spontaneous AMPA receptor-mediated synaptic transmission in mouse hippocampal CA1 area. *Eur. J. Neurosci.* *30*, 1559–1564.

SUPPLEMENTARY FIGURES

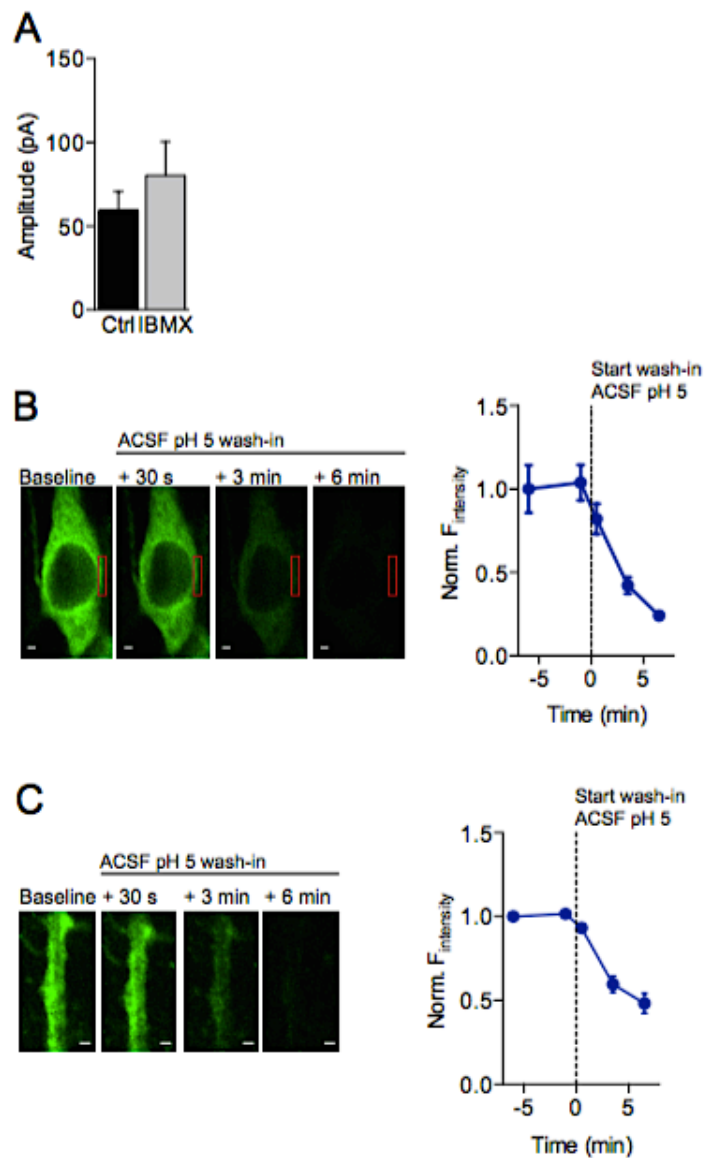


Figure S1. (A) Blocking phosphodiesterase activity with IBMX is not sufficient to induce AMPAR potentiation. Amplitudes of outside-out evoked recordings (from SEP-GluA3-positive neurons) in response to AMPA puffs in control condition or in the presence of IBMX. (B) Example images and average fluorescence intensity of SEP-infected GluA3-KO at the edge of cell bodies (top, $n=3$) or at apical dendrites (bottom, $n=3$) visualized with 2-photon laser scanning microscopy before and after wash-in of pH5-buffered ACSF ($n=3$). Error bars indicate SEM, scale bars indicate $5\ \mu\text{m}$, * indicates $p<0.05$.

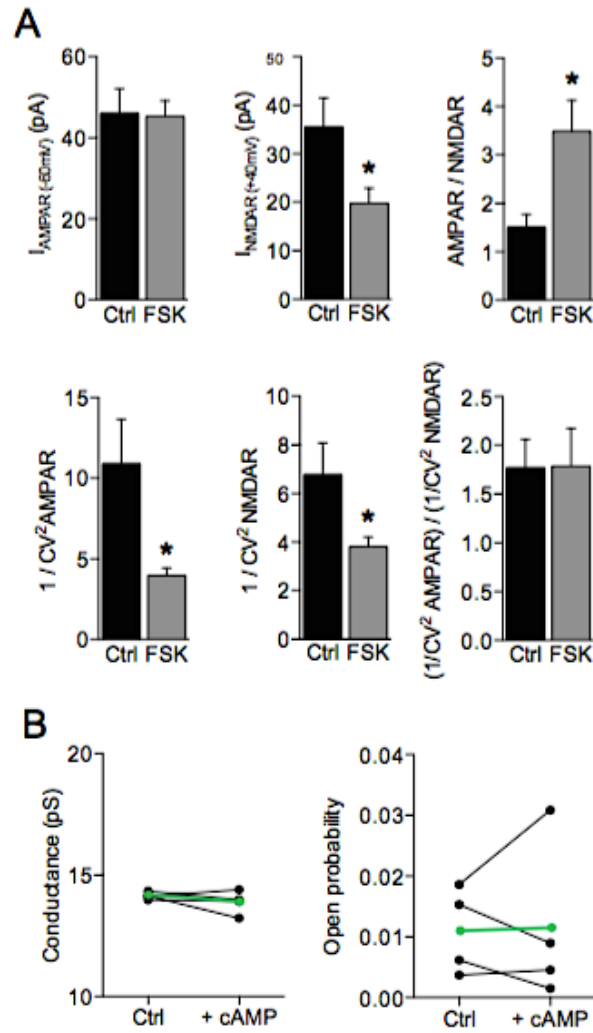


Figure S2. (A) Evoked AMPAR EPSC amplitude and quantal content ($1/\text{CV}^2$) of AMPAR EPSCs, average NMDAR EPSC, NMDAR $1/\text{CV}^2$, AMPAR/NMDAR EPSC ratio (as seen in figure 3B), and AMPAR/NMDAR $1/\text{CV}^2$ ratio, of WT CA1 neurons with or without forskolin. The quantal content depends on the quantal size and number of effective synapses, and correlates linearly with the inverse square of the coefficient of variation (CV^2) (Kerchner and Nicoll 2008). AMPAR responses of approximately 50 pA in amplitude were evoked while holding the CA1 neuron at -60 mV. When forskolin was present, the CV^2 was significantly lower ($p=0.001$), suggesting that stimulating fewer axons was sufficient to evoke AMPAR responses of the same amplitude. If GluA3-dependent plasticity would be expressed presynaptically, we would expect both AMPAR and NMDAR currents to be affected. However, when the same stimulation intensity was maintained at +40 mV to measure NMDAR responses, the low CV^2 in the presence of forskolin led to proportionally smaller NMDAR current amplitudes ($p=0.02$). Forskolin incubation did not change the relative quantal content measured from AMPAR and NMDAR responses ($p=0.7$), which suggests that the activation of GluA3-plasticity did not involve the unsilencing of synapses. (B) Direct stimulation of GluA3 does not activate GluA3-plasticity. Conductance (left) and open probability (right) of somatic inside-out recordings from GluA1-KO CA1 neurons with S-AMPA (100 μM) in the recording pipette, before and after puffing cAMP (100 μM) onto the patch. Error bars indicate SEM, * indicates $p<0.05$.

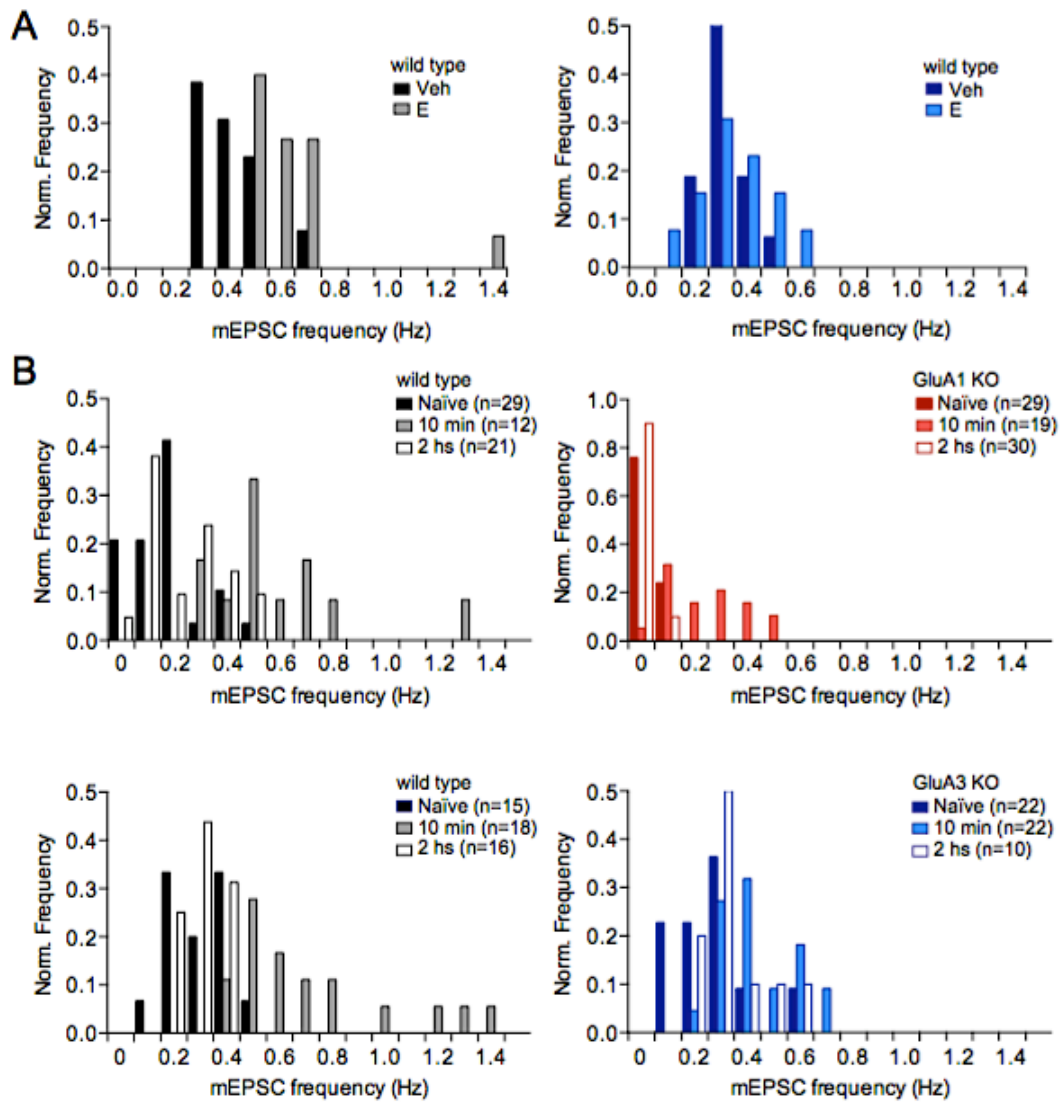


Figure S3. Glu3 plasticity is induced in the majority of CA1 neurons upon the injection of epinephrine or 10 min after fear conditioning. (A) Histograms of mEPSC frequencies from recordings of figure 5C. (B) Histograms of mEPSC frequencies from recordings of figure 6C and 7C respectively.

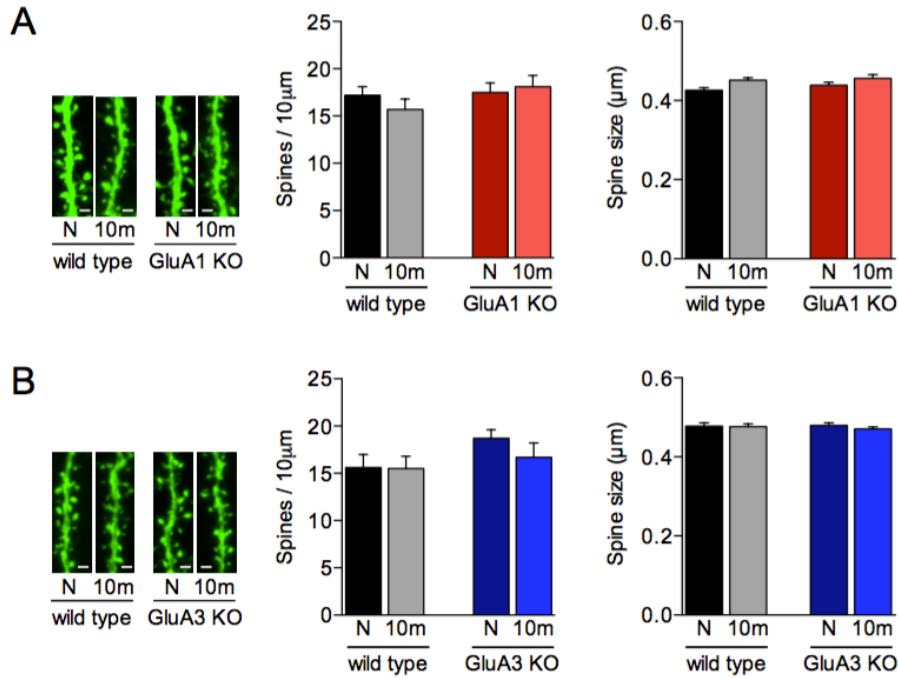


Figure S4. (A) Spine densities were counted on apical dendrites of Thy1-eYFP-expressing GluA1-KO CA1 pyramidal neurons (N: n=44(3), 10m: n=29(2)), WT littermate neurons (N: n=57(4), 10m: n=38(3)), GluA3-KO neurons (N: n=55 dendrites (5 mice), 10m: n=43(4)) and neurons of WT GluA3 littermates (N: n=32(3), 10m: n=43(4)) without or 10 minutes after fear conditioning. Scale bars indicate 1 µm. Error bars indicate SEM.

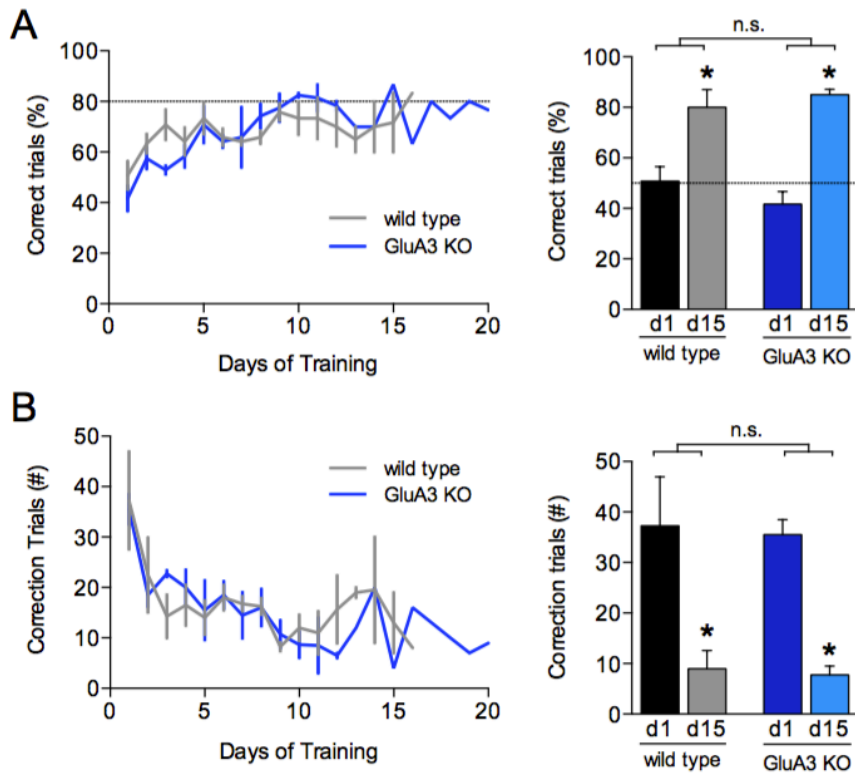


Figure S5. GluA3-KO mice (n=4) and wild type littermates (n=4) were trained in a reward based two-choice discrimination task. Mice were food restricted ($80 \pm 5\%$ of their normal weight) and daily trained for 60 trials or a maximum of 30 minutes. For every correct trial a reward (50 μ l of strawberry milkshake, Albert Heijn) was provided. Every incorrect trial was followed by a correction trial. After a score of 80% correct for three consecutive days the task was considered achieved. (A) Both GluA3-KO mice and wild type littermates significantly increased their percentage correct trials over the course of 15 days (WT: $p=0.023$; KO: $p=0.0007$). (B) Also, the number of errors decreased significantly over the course of the experiment (WT: $p=0.009$; KO: $p=0.009$), which indicates that the mice learned the task. However, no differences in performance were found between GluA3-deficient mice and wild type littermates after 15 days of training (Correct trials: $p>0.99$; Correction trials: $p>0.99$). Error bars indicate SEM, * indicates $p<0.05$.

EXPERIMENTAL PROCEDURES

Mice

GluA3-deficient (GluA3-KO) and wild-type littermate colony was established from c57bl6x129P2-Gria3tm1Dgen/Mmnc mutant ancestors (MMRRC, Davis, CA), which were at least 6 times backcrossed to c57bl6 mice. GluA1-deficient (GluA1-KO) mice were a kind gift from Dr. R. Huganir (Kim et al., 2005), and a colony was generated by mating heterozygous c57bl6/129 mice. For spine density experiments, mice were crossed to Thy1-eYFP transgenic mice (Porrero et al., 2010). GluA1xGluA3 double deficient colony was established by crossing homozygote GluA1-deficient males with heterozygote GluA3 females. Floxed GluA3 mice were a kind gift from Dr. R. Sprengel (Sanchis-Segura et al., 2006) and maintained in a homozygous colony. Mice were kept on a 12-hours day-night cycle (light onset 7am) and had *ad libitum* access to food and water. All experiments were conducted in line with the European guidelines for the care and use of laboratory animals (Council Directive 86/609/EEC). The experimental protocol was approved by the Animal Experiment Committee of the Royal Netherlands Academy of Arts and Sciences (KNAW).

Electrophysiology

Organotypic hippocampal slices were prepared from P7-8 mice as described previously (Stoppini et al., 1991) and used at 7-12 days in vitro. During recordings, slices were perfused with artificial CSF (ACSF, in mM: 118 NaCl, 2.5 KCl, 26 NaHCO₃, 1 NaH₂PO₄, supplemented with 4 MgCl₂, 4 CaCl₂, 20 glucose). Patch recording pipettes were filled with internal solution containing (in mM): 115 CsMeSO₃, 20 CsCl, 10 HEPES, 2.5 MgCl₂, 4 Na₂ATP, 0.4 Na-GTP, 10 Na-Phosphocreatine, 0.6 EGTA. Outside-out recordings were made with 3-5 M Ω pipettes and the bath contained the desensitization blockers PEPA (80 μ M; Tocris) and cyclothiazide (100 μ M; Tocris) to exclude variations due to differences in desensitization properties. Every 20 seconds a 100 ms puff of 100 μ M S-AMPA was delivered with a Picospritzer III (Parker, Hollis, USA). Single channel recordings were measured under cell-attached configuration with 6-8 M Ω pipettes filled with internal solution to which S-AMPA (100 μ M; Tocris) was added. Whole-cell recordings in organotypic slice cultures were made with 3-5 M Ω pipettes ($R_{\text{access}} < 20 \text{ M}\Omega$, and $R_{\text{input}} > 10 \times R_{\text{access}}$). During mEPSC recordings, TTX (1 μ M; Tocris) and picrotoxin (100 μ M; Sigma) were added to the bath. Where indicated, the following drugs were added to the perfusion solution: forskolin (50 μ M; Sigma), IBMX (50 μ M; Tocris), KT5720 (4 μ M; Tocris), PKI (2 μ M; Calbiochem), ESI05 (10 μ M; Biolog); Salirasib (10

μM ; Tocris); or inside the recording pipette: cAMP (100 μM ; Sigma), N002 (100 μM ; Biolog), 8-CPT (20 μM ; Tocris). Where indicated, slices were infected with Sindbis virus expressing GFP or SEP- tagged rat GluA3 (flip) 20-28 hours prior to experiments. During evoked recordings, a cut was made between CA1 and CA3, and picrotoxin (50 μM) and 2-chloroadenosine (4 μM ; Tocris) were added to the bath. Two stimulating electrodes, two-contact Pt/Ir cluster electrode (Frederick Haer), were placed between 100 and 300 μm down the apical dendrite, 100 μm apart, and 200 μm laterally in opposite directions. AMPAR-mediated EPSCs were measured as the peak inward current at -60 mV. NMDAR-mediated EPSC were measured as the mean outward current between 40 and 90 ms after the stimulation at +40 mV, and corrected by the current at 0 mV. Rectification was calculated as the ratio of the peak AMPAR current at -60 and +40 mV, corrected by the current at 0 mV, in the presence of D-APV (100 μM ; Tocris) in the bath and Spermine (0.1 mM; Sigma) inside the pipette. EPSC amplitudes were obtained from an average of at least 50 sweeps at each holding potential.

Acute hippocampal slices were prepared from 6 to 8 week-old mice when used for experiments involving fear conditioning and/or IP injections, or from 3 to 5 week-old mice when used for purely *in vitro* experiments. Dissection was done in ice-cold sucrose cutting solution containing (in mM): 2.5 KCl, 1.25 NaH_2PO_4 , 26 NaHCO_3 , 10 glucose, 0.5 CaCl_2 , 10 MgSO_4 , bubbled with 95% O_2 /5% CO_2 . Brain slices (400 μm) were cut using a vibratome (Thermo Scientific) and placed in a holding chamber containing ACSF supplemented with (in mM) 1 MgCl_2 , 2 CaCl_2 , 20 glucose and bubbled with 95% O_2 /5% CO_2 . They were allowed to recover at 34°C for 40 min then at room temperature for at least 40 min. Whole-cell recordings (3-5 $\text{M}\Omega$ pipettes, $R_{\text{access}} < 26 \text{M}\Omega$, and $R_{\text{input}} > 10 \times R_{\text{access}}$) were made in ACSF containing TTX (1 μM) and picrotoxin (50 μM) at 28°C. IBMX (50 μM ; Tocris) and isoproterenol (10 μM ; Sigma) were added to the perfusion solution where indicated.

Data was acquired using a Multiclamp 700B amplifier (Molecular Devices). mEPSC recordings were analyzed with MiniAnalysis (Synaptosoft). Individual events were manually selected, and an amplitude threshold of 5 pA was used. Evoked recordings were analyzed using pClamp 10 software (Molecular Devices). Non-stationary noise analysis of outside-out patches traces was carried out following previously described methods (Alvarez et al., 2002; Hartveit and Veruki, 2007). Peak aligned AMPA-evoked currents recorded over 10-15 sweeps per outside out patch, were binned in 10 equally sized bins of 150 ms each and for each bin, the mean amplitude and variance was calculated. The data distribution resulting after plotting amplitude

versus variance was fitted with the equation: $\sigma^2 = iI - \frac{I^2}{N} + \sigma_b^2$, where the variance (σ^2) of the amplitude of the current (I) obtained at each time point is explained as a function of the single unitary current (i) and the number of functionally conducting channels (N) with an offset given by the variance of the baseline noise (σ_b^2). From the derivative at $I=0$, the relative number of functional channels was extracted as well as the single channel conductance which was calculated by dividing the unitary current by the applied voltage with respect to the reversal potential ($V_{\text{holding}} - E_{\text{reversal}}$, -60mV and 0mV respectively). The peak open probability (P_0), corresponding to the fraction of available functional channels open at the time of the peak current (I_{peak}), is calculated with the equation: $P_0 = I_{\text{peak}}/N_{\text{max}}$, where N_{max} represents the theoretical maximum of available channels opened at the point where the theoretical maximum amplitude reaches the minimum variability (σ_b^2) in the given parabola fit. Single channel activity was analyzed using ClampFit. Three detection thresholds were used to detect O1 (1.5pA), O2 (3pA) and O3 (4.5pA) openings in single channel AMPARs in steady baseline recordings (no holding current fluctuations). Events with latency shorter than 0.3 ms were ignored to prevent noise from being recognized as openings.

Two-photon Laser Scanning Microscopy

Organotypic GluA3-deficient slices were sparsely infected with Sindbis virus expressing rat GluA3(flip) tagged with SEP, and were allowed to express for 20–28 hours. Three-dimensional images were collected on a custom-built two-photon microscope based on a Fluoview laser-scanning microscope (Femtonics). The light source was a mode-locked Ti:sapphire laser (Chameleon, Coherent) tuned at 910 nm using a 60x objective. Optical sections were captured every 1 μm from infected CA1 pyramidal cell bodies or apical dendrites past the point of bifurcation of primary to secondary dendrites, approximately 300 μm from the cell body. Fluorescence intensity was quantified from projections of stacked sections using ImageJ software (NIH).

Contextual Fear Conditioning Protocol and E-injection

For fear conditioning experiments, a box (29 cm high, 31.5 cm wide, 23 cm deep) with two metal walls, two transparent Plexiglas walls and grid floor with stainless steel bars through which the foot shock was delivered was used. The box was placed inside a sound-attenuating chamber (Med Associates Inc., Georgia, VT). The box was cleaned with 70% ethanol before each trial. During the training session, 6 to 8 weeks old mice were placed in the box. After 2 min, they were given 3 consecutive

shocks (0.80 mA for all experiments except Figure 7E: 0.65 mA, 1 sec duration, 1 min interval). They remained in the box 2 min after the last shock. For *in vitro* experiments either 10 minutes or 2 hours after the session the mice were decapitated and brain slices were obtained. For behavioral experiments mice were re-exposed to the fearful context at the specific time of testing. Freezing and motion were quantified using Matlab-based custom-made software (Kopec et al., 2007). To test generalization of fear memories the mice were put in two different contexts. The shock context was the regular fear conditioning box, cleaned with 70% ethanol. The neutral context was a modified version of the fear conditioning box. The walls consisted of circle-shaped white Plexiglas surrounding the walls, a white Plexiglas plate on the floor and the cage was cleaned with citric acid. For E injections (\pm)-Epinephrine hydrochloride (0.5mg/kg, Sigma-Aldrich) was dissolved in saline (0.9%, NaCl) and injected intraperitoneally (5ml/kg).

Stereotactic hippocampal viral injections

Three to four week-old mice were anesthetized with isoflurane (induction 5%, maintenance 2%) and positioned in a stereotaxic apparatus, kept on a heating pad. Bilateral hippocampal injections of viral solutions (3 injection sites per side; 400 nl per site; AP: -1.5, -1.7, -1.9; L: \pm 1.5; DV: 1.2 mm) were delivered with a glass micropipette through a hole drilled in the skull by pressure application (Nanoject II, Auto-Nanoliter Injector, Drummond Scientific). Experiments were performed at least 3 weeks after viral injections.

Spine Analysis

For spine density measurement Thy1-eYFP positive wild-type, GluA1-deficient or GluA3-deficient mice were anesthetized with pentobarbital and perfused with 20 ml 0.1 M PBS followed by 80 ml of fixative (4% paraformaldehyde in 0.1 M PBS, pH 7.2). Brains were removed, post-fixed for 1 hour in fixative, washed and stored in PBS at 4°C. Coronal 50 μ m-thick slices were prepared with a vibratome (Leica). They were mounted and covered with Vectashield mounting medium (Vector Labs). Z-stack images were made using a confocal microscope (Leica SP5) and analyzed with ImageJ software. Spine density was manually quantified and spine size (i.e. spinehead diameter) was measured from reconstructed dendrites (NeuroLucida, MBF Bioscience) made by an experimenter blind to experimental conditions and genotype.

Statistics

Data sets were Log-transformed and normal distributions were obtained. These were analyzed using two-tailed Student *t* tests to compare 2 conditions or ANOVAs with

post-hoc Tukey comparisons for comparing more than 2 conditions. *P* values below 0.05 were considered statistically significant.

REFERENCES

- Alvarez, O., Gonzalez, C., and Latorre, R. (2002). Counting channels: a tutorial guide on ion channel fluctuation analysis. *Adv. Physiol. Educ.* 26, 327–341.
- Hartveit, E., and Veruki, M.L. (2007). Studying properties of neurotransmitter receptors by non-stationary noise analysis of spontaneous postsynaptic currents and agonist-evoked responses in outside-out patches. *Nat. Protoc.* 2, 434–448.
- Kerchner, G.A., and Nicoll, R.A. (2008). Silent synapses and the emergence of a postsynaptic mechanism for LTP. *Nat. Rev. Neurosci.* 9, 813–825.
- Kim, C.-H., Takamiya, K., Petralia, R.S., Sattler, R., Yu, S., Zhou, W., Kalb, R., Wenthold, R., and Huganir, R. (2005). Persistent hippocampal CA1 LTP in mice lacking the C-terminal PDZ ligand of GluR1. *Nat. Neurosci.* 8, 985–987.
- Kopec, C.D., Kessels, H.W.H.G., Bush, D.E.A., Cain, C.K., LeDoux, J.E., and Malinow, R. (2007). A robust automated method to analyze rodent motion during fear conditioning. *Neuropharmacology* 52, 228–233.
- Porrero, C., Rubio-Garrido, P., Avendaño, C., and Clascá, F. (2010). Mapping of fluorescent protein-expressing neurons and axon pathways in adult and developing Thy1-eYFP-H transgenic mice. *Brain Res.* 1345, 59–72.
- Sanchis-Segura, C., Borchardt, T., Vengeliene, V., Zghoul, T., Bachteler, D., Gass, P., Sprengel, R., and Spanagel, R. (2006). Involvement of the AMPA receptor GluR-C subunit in alcohol-seeking behavior and relapse. *J. Neurosci.* 26, 1231–1238.